JBC Papers in Press. Published on April 5, 2018 as Manuscript RA117.000264
The latest version is at http://www.jbc.org/cgi/doi/10.1074/jbc.RA117.000264

Heparan sulfate antagonism alters bone morphogenetic protein signaling and receptor dynamics, suggesting a mechanism in Hereditary Multiple Exostoses

Christina Mundy[#], Evan Yang[#], Hajime Takano^, Paul C. Billings[#], and Maurizio Pacifici[#]

From the [#]Translational Research Program in Pediatric Orthopaedics, Division of Orthopaedic Surgery, and the ^Department of Pediatrics, Division of Neurology, The Children's Hospital of Philadelphia, Philadelphia, PA 19104

Running title: BMPR dynamics in HS deficiency

To whom correspondence should be addressed: Christina Mundy PhD, Translational Research Program in Pediatric Orthopaedics, ARC 904, 3615 Civic Center Blvd., Philadelphia, PA 19104. Tel.: 267 425 2077; Fax: 267-426-2215; E-mail: matticolac@email.chop.edu

Keywords: bone morphogenetic protein, heparan sulfate, cell surface receptor, signaling, cell biology and Hereditary Multiple Exostoses

ABSTRACT

Hereditary Multiple Exostoses (HME) is a pediatric disorder caused by heparan sulfate (HS) deficiency and is characterized by growth plate-associated osteochondromas. Previously, we found that osteochondroma formation in mouse models is preceded by ectopic bone morphogenetic protein (BMP) signaling in the perichondrium, but the mechanistic relationships between BMP signaling and HS deficiency remain unclear. Therefore, we used an HS antagonist (Surfen) to investigate the effects of this HS interference on BMP signaling, ligand availability, cell surface BMP receptor (BMPR) dynamics and BMPR interactions in Ad-293 and C3H/10T1/2 cells. As observed previously, the HS interference rapidly increased phosphorylated SMAD family member 1/5/8 levels. FACS analysis and immunoblots revealed that the cells possessed appreciable levels of endogenous cell surface BMP2/4 that were unaffected by the HS antagonist, suggesting that BMP2/4 proteins remained surface bound but became engaged in BMPR interactions and SMAD signaling. Indeed, surface mobility of Snap-tagged BMPRII, measured by fluorescence recovery after photobleaching (FRAP), was modulated during the drug treatment. This suggested that the receptors had transitioned to lipid rafts acting as signaling centers, confirmed for BMPRII via ultracentrifugation to separate membrane subdomains. *In situ* proximity ligation assays disclosed that the HS interference rapidly stimulates BMPRI-BMPRII interactions, measured by oligonucleotide-driven amplification signals. Our in vitro studies reveal that cell-associated HS controls BMP ligand availability and BMPR dynamics, interactions and signaling, and largely restrains these processes. We propose that HS deficiency in HME may lead to extensive local BMP signaling and altered BMPR dynamics, triggering excessive cellular responses and osteochondroma formation.

INTRODUCTION

Hereditary Multiple Exostoses (HME)[2] is a congenital autosomal dominant disorder –also known as Multiple Osteochondromas (MO)- in which benign cartilage-capped bony tumors form along the border between the growth plate and perichondrium in long bones, ribs, vertebrae, pelvis and cranial base in children and adolescents (1-4). Due to their location, large number and size, the tumors (called exostoses or osteochondromas) can cause numerous health problems, including skeletal deformities, growth retardation, blood vessel and nerve impingement, early onset osteoarthritis, and chronic pain (5,6). Most HME

cases are caused by heterozygous loss-of-function mutations in the Golgi-associated and heparan sulfate (HS)-synthesizing enzymes EXT1 or EXT2 (7-10), resulting in a partial systemic HS deficiency (11,12). It has long been assumed that osteochondroma formation is directly linked to HS loss, but a complete understanding of the nature of how this manifests into a pathogenic disorder is still unknown (13).

The HS chains are components of critical cell surface- and extracellular matrix-associated proteoglycans (HSPGs) that regulate numerous developmental and physiologic mechanisms and processes and in particular, the topography, range of action and signaling activity of bone morphogenetic proteins (BMPs), fibroblast growth factors (FGFs) and other HS-binding signaling proteins (14-17). Indeed, we showed in previous studies that conditional *Ext1*$^{f/f}$ ablation and ensuing severe decrease in HS levels caused ectopic canonical BMP signaling in long bone perichondrium in mouse models of HME (18). The induction of BMP signaling in perichondrium was followed by a phenotypic switch in resident cells from mesenchymal/fibroblastic to chondrogenic and by formation of cartilaginous osteochondroma-like tissue masses over time. Our studies revealed for the first time that locally enhanced BMP signaling is a major culprit in osteochondroma induction and growth and that the tumors originate from perichondrium-associated stem and progenitor cells (13,18). In very good agreement with these key findings, we showed in a more recent study that systemic administration of the BMP signaling antagonist LDN193189 markedly reduced osteochondroma formation in the HME mouse models (3), representing the first demonstration ever that osteochondroma formation is amenable to drug treatment. A study confirming our data has just been published (19). Together, the data indicated that a critical role of HS within developing and growing skeletal elements is to curb BMP action and signaling, possibly by limiting BMP availability and interactions with BMP receptors (BMPRs). Thus, aberrant function of these mechanisms resulting from decreases in HS levels can be pathogenic.

It is well established that cell surface BMPRs are tetrameric complexes each composed of two type I receptors (BMPRIa or BMPRIb) and two type II BMP receptors (BMPRII, ACVR2a and ACVR2b) that transduce BMP action by mainly signaling via canonical phosphorylated SMAD1/5/8 proteins (20-23). Of particular relevance here are studies performed by Knaus and colleagues in which they analyzed and characterized the mechanisms of BMPR signaling in various types of cells in vitro (24-27). In particularly probing studies, they made use of combinations of high resolution, live-cell imaging techniques and biochemical assays to investigate BMPR mobility, interactions and signaling kinetics. They found that BMPRI and BMPRII have distinct mobility patterns under unstimulated conditions, and that the highly mobile BMPRII population became immobilized and bound to BMPRI during rhBMP2 treatment. Data with C2C12 cells indicated that upon treatment with exogenous rhBMP2, the mobility of the BMPRII population was quickly reduced and the receptors were recruited into lipid rafts where they oligomerized with the resident BMPRI population, eliciting canonical SMAD signaling (25).

Because of its potency and multiple regulatory functions, BMP signaling needs to be highly regulated (28-30). As pointed out above, BMP family members all possess a high affinity and specific HS-binding domain and thus, it is likely that their interactions with HS chains and HSPGs represent an important mechanism of regulation of BMP biological action (14,17). However, details remain unclear. Kuo et al. analyzed the role of HS in the signaling activity of recombinant BMP2 and BMP4 in C2C12 and PC12 cell cultures (31). They found that when the cells were pre-treated with heparitinase, their response to exogenous BMPs and canonical signaling were diminished, accompanied by a reduction in BMPRI/II oligomerization as revealed by protein cross-linking, immunoprecipitation and fluorescence correlation microscopy. In related studies, Jiao et al. (32) and Manton et al. (33) observed that heparitinase treatment actually enhanced BMP signaling and osteogenic cell differentiation in response to exogenous BMPs. Similarly, we observed in mouse embryo limb mesenchymal cells in high density micromass cultures that chondrogenic cell differentiation and

canonical BMP signaling were greatly stimulated by treatment with heparitinase, heparanase or the HS antagonist Surfen, in the absence of exogenous BMPs (18,34). Others found that recombinant BMP2 and BMP4, in which the HS-binding region was mutated and non-functional, exhibited higher activity in cultured cells and a broader and stronger action in vivo as measured by *Xenopus* embryo ventralization assays (35,36). Together, current evidence points to the overall conclusion that HS and HSPGs exert complex regulatory roles in BMP and BMPR function. They appear to be needed to capture and retain BMPs and can then exert positive or negative modulation of BMP signaling activity in distinct contexts and processes.

In the present study, we have interrogated these mechanisms in greater detail and specifically asked to what extent HS regulates mobility, dynamics, interactions and signaling of BMPRIa and BMPRII members. To do so, we used live cell imaging, fluorescence-recovery after photobleaching (FRAP), FACS and other biochemical tests in cultured cells and analyzed and measured those parameters before and after acute HS interference. For the latter, we used Surfen to modulate HS function rather than content or structure. The data provide strong evidence that a main role of cellular HS is to limit BMP signaling and BMPR dynamics, suggesting that alterations of such basic restraining mechanisms during severe HS deficiency could be deleterious and promote cell misbehavior and disease progression.

RESULTS

HS interference elicits increases in endogenous BMP activity and SMAD signaling - To assess the roles of HS in regulating BMP signaling in manners reflective of cellular homeostatic and dynamic mechanisms, we initially carried out studies on endogenously expressed ligands and receptors. Thus, we first determined the steady-state levels of gene expression of representative BMPs and BMPRs in Ad-293 and C3H/10T1/. The cell lines used here are popular and have been used in numerous studies, including those dealing with pediatric skeletal diseases (37,38). RT-PCR analysis showed that both cell lines displayed readily detectable levels of transcripts encoding *Bmp2*, *Bmp4, BmpRIa* and *BmpRII* (Supplemental Fig. 1*A* and *B*) as well as those for the BMP early response target gene *Id1* (Fig. 1*A* and *B*). Both cell lines also exhibited appreciable basal levels of phosphorylated SMAD1/5/8 (pSMAD1/5/8) (Fig. 1*C* and 1*E,* lane 1) that were quickly enhanced several fold within 15 min of treatment with rhBMP2 and remained so for at least 1 h (Fig. 1*C, G, E and I,* lanes 2-6). The above data indicated that both cell lines had a basal level of BMP signaling and were able to adjust and increase it upon changes in ligand availability. To determine the extent to which HS regulated such basal levels of BMP signaling, the cells were treated with Surfen and processed for analysis and quantification of the above parameters. In previous studies using analytical tools including surface plasmon resonance, we and others showed that Surfen competes with protein factor binding to HS and can dislodge BMPs pre-bound to HS (18,39). In good agreement, we observed that Surfen provoked a clear increase in pSMAD1/5/8 levels within 30 min of treatment in Ad-293 cells, amounting to over 4.0 fold by 1 to 2 h (Fig. 1*D*, *H,* lanes 2-6). Similar responses occurred in C3H/10T1/2 cells, but were slower (Fig. 1*F, J* lanes 2-6). Surfen treatment also elicited a strong stimulation of *Id1* expression (Fig. 1*A* and *B*). Notably and importantly, the drug-induced responses were largely prevented by co-treatment with recombinant Noggin, a potent BMP antagonist (Supplemental Fig. 2) (40). In addition, Noggin treatment decreased: (i) basal *Id1* expression and rhBMP2-induced *Id1* overexpression (Supplemental Fig. 2*A-C)* and (ii) basal, rhBMP2-induced and drug-induced pSMAD1/5/8 levels (Supplemental Fig. 2*D-G)*. In sum, the above data indicate that basal levels of BMP signaling in Ad-293 and C3H/10T1/2 are readily increased following functional interference with HS. Because such responses were counteracted by Noggin co-treatment, they likely reflected an increase in availability and activity of endogenous ligands at the cell surface.

To strengthen the latter conclusion, we directly investigated the possible presence of BMPs on the cell surface, using fluorescent-activated cell sorting (FACS). Ad-293 cells were

lightly fixed with formaldehyde (and thus still impermeable), were incubated with primary rabbit BMP2/4 antibodies followed by secondary AlexaFluor-488-labeled antibodies, and were finally subjected to FACS. Companion cells pre-treated with Surfen for 1 h were processed at the same time. Both cell populations produced strong signal patterns consisting of a prominent fluorescence peak at intensity 10^5-10^6 preceded by a small peak at about 10^4 likely representing background signal (Fig. 2*D* and *E*). Relative fluorescence values for both populations were extremely strong (Fig. 2*F*, 1°+2° abs and 1°+2° abs + Surfen). To test specificity, companion cells were fixed, incubated with (i) vehicle, (ii) secondary antibodies only or (iii) primary pre-immune rabbit antibodies followed by fluorescent-labeled secondary antibodies, and subjected to FACS. Vehicle-treated cells elicited a narrow peak of background fluorescence around intensity 10^3 (Fig. 2*A*), and cells reacted with secondary antibodies only or primary pre-immune plus secondary antibodies produced broader fluorescence patterns below intensity 10^5 (Fig. 2*B* and *C*). The relative fluorescence values for these control populations were far lower (Fig. 2*F,* no 1° and 2° abs, 2° only and preimmune 1° ab + 2° ab) than those elicited by cells exposed to primary immune and secondary antibodies (Fig. 2*F*, 1°+2° abs and 1°+2° abs + Surfen). When Ad-293 cells were pre-treated with trypsin for 15 min, fixed and then reacted with primary immune and secondary antibodies, their fluorescence signal was drastically reduced (Fig. 2*F*, trypsin-treated conditons), indicating that BMP2/4 were surface-bound and susceptible to protease digestion. To further double-check the data, untreated cells and companion cells treated with Surfen for 1 h were processed for immunoblot analysis of endogenous BMP2, using a rabbit monoclonal antibody. Indeed, both populations elicited a single prominent immunoreactive band of approximately 15kDa (Fig. 2*G*) under reducing conditions and present in similar relative amounts in both cell populations (Fig. 2*H*). Together, the above lines of experimentation indicate that Ad-293 cells do possess endogenous cell surface-bound BMP2 and/or BMP4. The apparent protein levels do not substantially change after acute drug treatment, suggesting that Surfen did not dislodge the proteins away from the surface but likely made them available for BMPR interactions and signaling (see Fig. 1).

BMPR mobility and association with lipid rafts change upon HS interference - Given that BMP signaling and pSMAD1/5/8 levels increased readily after Surfen treatment, we asked whether these responses were associated with, and likely due to, changes in BMPR mobility and clusterization into lipid rafts (41). For these analyses, we resorted to live cell imaging during fluorescence recovery after photo-bleaching (FRAP) and created BMPR-fusion protein expression constructs, using the SNAP-tag technology (42,43). This approach has significant advantages over traditional methods, including the fact that the tag can be labeled with diverse non-permeant fluorophores and is small, thus likely to interfere less, or not at all, with fusion protein's routing and destination through cellular compartments including endoplasmic reticulum, Golgi and cell surface. Accordingly, Ad-293 cells were transfected with *Snap-BMPRIa* or *Snap-BMPRII* expression plasmids for 48 hours after which the cells were labeled with fluorescent SNAP surface-tag 488. Live cell imaging revealed very strong and clear fluorescence signal with either construct that was almost exclusively restricted to the cell surface (Fig. 3*A* and *C*) that - as pointed out above- likely reflected a seemingly normal handling of the fusion proteins through secretory and cell surface machinery without abnormal accumulation in intracellular compartments. Additionally, we collected lysates of cells transfected with empty Snap vector, *Snap-BMPRIa* or *Snap-BMPRII* expression plasmids and found that each cell population expressed the respective protein of appropriate molecular weight (Supplemental Fig 3*A-C*). To demonstrate that the presence of the fusion proteins did not alter BMP signaling and may actually render the cells more responsive, Ad-293 cells were co-transfected with both *Snap-BMPRIa* and *Snap-BMPRII* constructs, treated with indicated agents for various time lengths, lysed and processed for RNA and protein analyses. Treatment with exogenous rhBMP2 greatly up-regulated *Id1* gene expression and did

so by over 10-fold over vehicle-treated cells (Fig. 3*B*). A similar over-response was seen after Surfen treatment that upregulated *Id1* gene expression by more than 3-fold (Fig. 3*B*). Incubation with rhBMP2 or drug also increased pSMAD1/5/8 protein levels by over 4- and 3-fold, respectively, compared to control vehicle-treated cells (Fig. 3*D* and *E*). However, when the co-transfected cells were treated with rhBMP2- or Surfen in the presence of Noggin, the increases in *Id1* expression failed to occur (Fig. 3*B*). Noggin treatment by itself reduced the baseline levels of *Id1* expression (Fig. 3*B*).

To assess and quantify lateral BMPR mobility, Ad-293 cells transfected with *Snap-BMPRII* or *Snap-BMPRIa* plasmid constructs were labeled with Snap surface tag 488 (Fig. 4*A* and 5*A*) and processed for FRAP assays. Cells were initially subjected to a 200 millisec (ms) laser pulse to bleach representative areas of the cell surface (Fig. 4*B* and 5*B*, yellow box), and images were then acquired at regular intervals to monitor and calculate fluorescence recovery over time up to 250 sec, in the absence or presence of exogenous rhBMP2 or Surfen (Fig. 4*C-E* and 5 *C-E*). In cells expressing *Snap-BMPRII*, acute treatment with rhBMP2 caused a significant increase in halftime recovery time ($\tau 1/2$) compared to vehicle-treated control cells, from an average $\tau 1/2 = 33.89$ sec in the latter to about $\tau 1/2 = 52.08$ sec after rhBMP2-treatment (Fig. 4*F* and *G*). A comparable and significant increase in $\tau 1/2$ recovery was seen in companion *Snap-BMPRII*-expressing cells acutely treated with Surfen (Fig. 4*H*; $\tau 1/2 = 54.99$ sec). Data obtained from 30 individual cells from 3 independent experiments showed that differences in $\tau 1/2$ in control vs treated cells were highly reproducible and statistically significant (Fig. 4*I*). In good correlation, the changes in $\tau 1/2$ recovery brought about changes in BMPRII mobile fraction population (Fig. 4*J*). This trend was obvious in both rhBMP2- and drug-treated cells, but reached statistical significance only in the latter. Notably, when the cells were treated with rhBMP2 or Surfen in the presence of Noggin, $\tau 1/2$ was significantly reduced in both treated cultures (Supplemental Fig. 3*D,E, G and H*). This was accompanied by a slight increase in mobile fraction in the rhBMP2 plus Noggin and Surfen plus Noggin treated cells (Supplemental Fig. 3*F* and *I*). The data suggested that Noggin maintained the mobility of BMPRII population. Because Noggin treatment by itself did not have major effects on BMPRII mobility (Supplemental Fig. 2*A-C*), changes in those parameters in drug-treated cells were likely due to increased availability or activity of endogenous BMPs.

Different observations were obtained in *Snap-BMPRIa*-expressing cells (Fig. 5). Treatment with rhBMP2 or Surfen did not appreciably alter the $\tau 1/2$ recovery or mobile receptor fraction population compared to levels seen in vehicle-treated cells (Fig. 5*F-J*). As above, we analyzed 20-30 cells in multiple independent experiments, and data were highly consistent and reproducible. Thus, at variance with the changes in BMPRII mobility and dynamics following acute exposure to rhBMP2 or Surfen, it appears that the BMPRIa population is rather static and is not affected in major manners by HS interference or exogenous ligands.

The significant decrease in BMPRII lateral mobility triggered by drug treatment above likely indicates that this receptor had been recruited to lipid raft domains well known to serve as centers for receptor oligomerization and signal transduction (41). To test this prediction, we determined the distribution of SNAP-BMPRII and SNAP-BMPRIa in detergent-resistant membranes (DRMs), which are mainly composed of lipid rafts (44,45). Accordingly, Ad-293 cells expressing *Snap-BMPRII* or *Snap-BMPRIa* were treated with Surfen or vehicle for 10-15 min and extracted with nonionic detergents, and the resulting cell extracts were processed for DRM fractionation by sucrose gradient ultracentrifugation (44,45). Gradients were subdivided into consecutive fractions, and proteins in each fraction were separated and analyzed by gel electrophoresis and immunoblots. Caveolin-1 was used as marker of lipid rafts (41,46). In vehicle-treated control cells, the SNAP-BMPRII population was detectable in both DRMs and non-DRMs (fractions 2-8) whereas caveolin-1 resided mostly in DRMs as expected (fractions 1-5) (Fig. 6*A*). Interestingly, in drug-treated cells, there was a clear shift in the

distribution of SNAP-BMPRII that was now most abundant in the DRMs (fractions 1-5) (Fig. 6*C*), indicating that a significant portion of the receptor population had shifted to lipid rafts (Fig. 6*E*). In comparison, in vehicle-treated control cells, SNAP-BMPRIa was mainly detected in the DRMs (fractions 1-4) (Fig. 6*B,F*) and remained largely confined to the DRMs after Surfen treatment (fractions 1 through 5). A small percentage of population was present in the non-DRMs (fractions 6-8) (Fig. 6*D,F*).

HS interference leads to increased interactions between BMPRIa and BMPRII - The data above indicate that interference with HS promoted the recruitment of the BMPRII to lipid rafts where they would presumably interact with resident BMPRIa to elicit an increase in BMP signaling (see Fig. 6). To obtain more direct evidence of changes in BMPRII/BMPRIa interactions upon HS interference, we carried out proximity ligation assays (47,48). Ad-293 and C3H/10T1/2 cells were first treated with Surfen, rhBMP2 or vehicle for 10 to 15 min and fixed. After blocking, the cells were incubated with oligonucleotide-containing antibodies to BMPRIa or BMPRII, rinsed and incubated with a hybridization solution containing connector oligomers binding to their respective antibodies. This was followed by ligation and amplification in the presence of a 594 fluorophore, generating bright red fluorescence dots on the cell surface indicative of closely-associated and interacting proteins (47,48). Vehicle-treated cells displayed a basal number of red fluorescence dots that were uniformly distributed over the cell surface (Fig. 7*A*, *E*, *I* and *M*). Microscopic inspection and image-based quantification of at least 30 cells in three separate experiments showed that control cells had an average of about 45 detectable dots/cell in Ad-293 cultures and about 30 detectable dots/cell in C3H/10T1/2 cultures (Fig. 7*Q* and *R*). Strikingly and clearly, an acute treatment (10-15 minutes) with rhBMP2 or Surfen led to a sharp increase in the number of fluorescent dots that was quite apparent and obvious by simple microscopic inspection (Fig. 7*B, F, J* and *N* and *7C, G, K* and *O*, respectively) and was confirmed by quantification and statistical analyses (Fig. 7*Q* and *R*). To demonstrate that these receptor interactions were in fact due to ligand availablilty, we preincubated rhBMP2 with noggin or Surfen with noggin for 10 minutes at 37°C. We then applied the rhBMP2/noggin and Surfen/noggin mixtures (or noggin alone) to the cells for 10-15 minutes. PLA was carried out and indeed, we found that noggin prevented rhBMP2-induced (Supplemental Fig. 5*B, E* and *G*) and drug-induced (Supplemental Fig. 5*C, F* anf *G*) BMPRIa and BMPRII interactions compared to BMP2 and Surfen alone (Fig. 7). Companion cultures exposed to pre-immune antibodies (same species, same dilution) and then processed for the entire proximity ligation procedure elicited no detectable signal (Fig. 7*D*, *H, L* and *P*), attesting to specificity of procedure.

DISCUSSION

As many other members of key signaling protein families (14,17), BMPs have long been known to possess a HS-binding domain (36), but importance and functional roles of the resulting HS-BMP interactions on BMPR action have remained poorly understood. The in vitro data we present here provide a series of compelling and interconnected observations leading to the overall conclusion that HS has a clear role in regulating the dynamic behavior of BMPRs and in modulating BMP signaling. Based on cellular responses detailed above, it appears that HS largely has a restraining influence on BMP activity and signaling and that its functional deficiency leads to increased signaling. Given that these responses are appreciable in the absence of exogenously provided BMPs, they clearly reflect mechanisms engaging resident endogenous ligands and receptors and importantly, their native stochiometries and dispositions. Admittedly, the signaling responses to drug treatment are slower than those elicited by exogenous rhBMP2 treatment and are also smaller in scale. However, exhuberant responses to exogenous BMPs are likely to be unrealistic and above physiological levels, given that even at nanomolar rhBMP2 doses used here and previous studies, such doses are bound to be vastly higher than those of endogenous ligands (likely including active and precursor forms). Together, our data suggest that

the cell surface of Ad-293 and C3H/10T1/2 cells contains native BMPs interacting with HS and potentially available for action, becoming engaged in signaling upon modulation of HS restraining influence (Figure 8).

Cell surface receptors are highly dynamic entities, can move in and out of lipid rafts, and can establish functional interactions with their respective partners and appropriate ligands to signal (49,50). The BMPRs conform to these general trends and as indicated above, different BMPRs examined so far have been found to have distinct cell surface translocation dynamics and distribution. In cells such as C2C12, a large portion of the BMPRIa population resides in lipid rafts and is rather static, whereas the BMPRII population is highly dynamic and seemingly distributed more broadly on the surface (20,25,26). The BMPRIIs quickly transition to lipid rafts upon acute treatment with rhBMP2 or rhBMP4. Our data with rhBMP2-treated Ad-293 and C3H/10T1/2 cells largely agree with those observations, implying that the differential dynamics and distribution of BMPRII versus BMPRIa may reflect fairly general cellular characteristics and that the recruitment of BMPRII to lipid rafts may set the overall degree of signaling. Our data, however, provide the first demonstration ever that a similar physical re-arrangement of the receptors occurs upon functional interference with HS in the absence of exogenous rhBMPs. Because signaling eventually follows such receptor redistribution, the data imply that the dynamic response of the receptors to HS deficiency and their direct interactions were fruitful and productive and led to downstream effector action. It is important to note here that our data only explores one of the three type II BMP receptors, therefore it is unknown whether ACVR2a or ACVR2b would behave in a similar manner to BMPRII. The data are in line with the possibility raised above that the Ad-293 and C3H/10T1/2 cells possess a reservoir of endogenous cell surface BMPs which can be recruited and engaged in signaling action upon modulation of HS influence. This notion is supported by the fact that signaling in response to Surfen was prevented by Noggin co-treatment, strongly indicating that the endogenous ligands were accessible to –and blocked by- such external protein antagonist. Our FACS data also are in line with that notion by showing that cell surface BMP2/4 were accessible to their antibodies, elicited a highly specific fluorescence signal and were susceptible to protease degradation in live cells. Because the FACS profiles did not change substantially after Surfen treatment, the data do indicate that the treatments did not dislodge a significant amount of endogenous ligands from the surface, instead presumably making them available for interactions and signaling with resident BMPRs.

Cell surface BMPR dynamics have been previously studied by FRAP as well as FRET and protein cross-linking and immunoprecipitation, but not by proximity ligation. A major advantange of this procedure is that it provides direct visualization of endogenous protein-protein complexes and their distribution and composition within individual cells, including between cytoplasmic proteins or transcription factors such as c-Myc and Max (47,48). Measurements and computation have indicated that the complexes reflect interacting proteins at an average distance of 10 to 20 nm from each other. In line with pSMAD1/5/8 levels reflective of basal BMP signaling (in the absence of exogenous BMPs), untreated control Ad-293 and C3H/10T1/2 cells displayed an appreciable number of BMPRIa/BMPRII complexes on their surface depicted by the red fluorescence amplification spots. Within a 10 to 15 min treatment with rhBMP2, the red spot number increased sharply as did after Surfen treatment (again without exogenous rhBMP2). Because rhBMP2 treatment caused a higher increase in spot number and higher pSMAD1/5/8 levels compared to Surfen treatment, the data raise the interesting possibility that there is a fairly direct correlation between number of surface BMPR complexes and degree and levels of BMP signaling, without a need to invoke changes in catalytic capacity of each complex depending on treatment type or experimental condition. As in the case of data from FRAP or FRET analyses (25-27), the increases in complex numbers revealed by the ligation assays occurred within minutes of Surfen treatment, in line with the highly dynamic nature

of cell surface receptors in response to ligands becoming acutely available. We should consider the possibility, however, that HS may have additional influences on the physical behavior of BMPRs and their signaling activity. BMPRs do not possess a stereotypic HS-binding domain (14), but it is possible that they may establish links to HS and HSPGs via intermediaries or with the PG core proteins. For instance, the core proteins of Syndecan-1 and Syndecan-2 were shown to interact with integrins and the tyrosine phosphatase receptor CD148 on the cell surface (51,52). In addition, HS is an integral component of the FGF/FGFR signaling complexes and is required for FGF signaling (53,54). In addition, Surfen may have influenced other glycosaminoglycans (39). Considered together, our data and previous studies point to the overall notion that HS may often -if not always- be involved in regulating protein signaling by influencing ligand availability and cell surface receptor dynamics and function, though in distinct and even opposing manners and depending on receptor types, signaling nature and cell types and context.

The above conclusions and putative scenarios are in agreement with the studies by Jiao et al. (32) and Manton et al. (33) indicating that BMP signaling and osteogenic cell differentiation increased in response to treatment with heparitinase and rhBMPs (55). They also agree with studies showing that recombinant BMP2 and BMP4 lacking a functional HS-binding region exhibited greater activity in cultured cells and a broader and stronger action in vivo as measured in *Xenopus* embryos (35,36). Together with the data here and our previous work on limb bud chondroprogenitor cells (18), current evidence does sustain the notion that HS largely limits BMP signaling in many/most contexts. However, this notion appears to be in sharp contrast with the observations by Kuo et al. (31) indicating that heparitinase pre-treatment greatly diminished BMP signaling and BMPR interactions in PC12 and C2C12 cells in response to exogenous rhBMP2. One admittedly trivial explanation of these divergent observations is that different cell culture techniques, media, recombinant protein purity and other factors may have influenced cell behavior and responses and thus, experimental outcomes. A more interesting explanation is that the data are actually reconcilable, but we need to take into account whether exogenous BMPs were used and whether short- or long-term responses were analyzed. Thus, in the Kuo et al. study, the pre-treatment with heparitinase may have decreased the ability of the cells to acutely "capture" the rhBMP2 added to the culture medium, leading to reduced pSMAD1/5/8 levels within the 1 hr period of analysis compared to heparitinase un-treated cells. On the other hand, the positive effects of heparitinase treatment on osteogenic cell differentiation may reflect lower but prolonged responses to exogenous rhBMP2, eliciting beneficial differentiation effects long-term. In the case of chondrogenic differentiation we studied in the absence of exogenous BMPs, the beneficial effects of Surfen or heparitinase would also reflect slow, low but sustained stimulation of BMP signaling. In sum, HS and HSPGs likely have multiple and interconnected roles in the regulation of BMP and BMPR signaling. They appear to be needed to capture BMPs and retain/preserve them on the cell surface, making them readily available for signaling upon perturbation of HS restraining function.

The observations here provide possible insights into the cellular pathogenesis of HME. It has long been known that the hererozygous loss-of-function mutations in *EXT1* or *EXT2* present in HME patients cause a systemic deficiency in HS levels of about 50% (11). This partial deficiency can in itself provoke certain physiologic abnormalities, including substandard lipid clearance and pancreas function (56,57). However, it is not sufficient to cause formation of osteochondromas that underlie the more severe health problems in HME patients, including skeletal deformations, chronic pain and even malignancy. In line with Knudson's law of tumorigenesis (58), osteochondroma formation requires a "second hit" such as loss-of-heterozygosity or other genetic changes that would lead to a steeper local drop in HS levels, as previous studies from our group and others have demonstrated (59-62). But how would such steep drop in HS lead to osteochondroma formation?

Because the tumors invariably form next to the growth plate of long bones and other skeletal elements in children and adolescents, we reasoned that perichondrium flanking the growth plates could be a key pathogenic player (18). Indeed, we showed that conditional ablation of both *Ext1* alleles in mouse models of HME led to: steep local loss of HS; changes in perichondrial cell phenotype; ectopic BMP signaling and chondrogenesis; and initiation of osteochondroma formation. Interestingly (and in line with the observations here), we observed the same chronological and phenotypic changes when wild type mouse long bone explants in organ culture were treated with Surfen or heparitinase (18). Both treatments caused a prominent induction of ectopic BMP signaling in perichondrium (as indicated by pSMAD1/5/8 levels) that was followed by ectopic chondrogenesis and osteochondroma-like tumor formation. These responses were absent in companion vehicle-treated controls. Thus and as strongly indicated by the data in the present study, it is possible that under normal conditions, HS in perichondrium would restrain the activity of BMPs that are expressed in that tissue (63-65), preventing them from exerting their notorious pro-chondrogenic action and allowing the perichondrium to maintain its normal fibroblastic and mesenchymal character. A local steep drop in HS levels or function would, however, liberate BMPs, allow them to interact with their receptors, elicit canonical BMP signaling, and trigger ectopic chondrogenesis and osteochondroma initiation. Notably, perichondrium possesses additional mechanisms that normally protect and sustain its mesenchymal character, including anti-chondrogenic factors and pathways such as FGFs and FGF signaling mediators ERK1/2 (40,66). The steep local drop in HS leading to osteochondroma initiation would thus need to alter such mechanisms as well. Given that FGF signaling actually requires HS, it is possible that a severe local HS deficiency in HME could cause a decrease in FGF-dependent anti-chondrogenic action and a reciprocal increase in BMP-dependent pro-chondrogenic action, a combination of responses that could converge to promote ectopic chondrogenesis and osteochondroma formation. It is important to point out that these novel findings should be extended in cell types that are relevant to HME to fully understand the mechanisms of pathogenesis.

EXPERIMENTAL PROCEDURES

Construction of Snap-BMPRIa and Snap-BMPRII plasmids – Design and construction of these fusion protein vectors were based on previous studies (42,43). *BMPRIa* and *BMPRII* cDNA clones and the $pSnap_f$ vector were purchased from Origene and New England Biolabs, respectively. The $pSnap_f$ vector has two multiple cloning sites that flank the N and C terminal ends of the SNAP protein. Thus, we designed primers to amplify the signal peptide with restriction enzymes NheI and EcoRI and mature peptide with restriction enzymes BamHI and NotI of the receptors (Supplemental Table 1). After electrophoresis, we cut and purified the inserts. To insert the signal peptide of the receptors into the $pSnap_f$ vector, we first, digested the vector with NheI and EcoRI then inserted the signal peptide via ligation using the Quick Ligation Kit according to the manufacturer's protocol (New England Biolabs). After transformation, colonies were selected and subjected to PCR to identify positive colonies for the signal peptide. Those colonies were further amplified and purified. The newly constructed plasmids, RIA signal peptide-Snap and RII signal peptide-Snap were cut with BamHI and NotI. The inserts of the mature peptide of the receptors were ligated and transformed. The transformed coloines were selected, subjected to colony PCR and purified. In sum, for *Snap-BMPRIA*, the Snap-tag is positioned after the glutamine residue (position 22 - end of the signal peptide) and before glycine (position 23 - start of the mature peptide). For *Snap-BMPRII*, the Snap-tag is positioned after the alanine residue (position 25 – end of the signal peptide) and before alanine (position 26 – start of the mature peptide). The final plasmids, referred to as *Snap-BMPRIa* and *Snap-BMPRII*, were submitted to our Nucleic Acid and Protein Core Facility to verify sequencing and construction.

Protein Analysis in cell cultures - Ad-293 cell line, a derivative of the commonly used HEK 293 cell line with improved adherence, was

purchased from Agilent Technologies and the C3H/10T1/2 cell line was purchased from ATCC. Cells were grown in monolayer and transfected with *Snap-BMPRIa* and/or *Snap-BMPRII* or left untransfected. Transfection was carried out using Fugene 6 (Promega) reagent according to the manufacturer's protocol. Briefly, cells grown in 6 well plates for protein analysis were transfected with 1 μg of plasmid and 3 μl of Fugene 6 reagent per well in 10% FBS/DMEM and incubated for 24-48 hours. Following transfection, the media was changed to 0.1% BSA/DMEM, and the next day the cells were treated with vehicle (control), recombinant human (rh)BMP2 (25 ng/ml; Gemini Bioproducts), Surfen (5 μM; Open Chemical Repository: NSC 12155), Noggin (50 ng/ml; R&D Systems), rhBMP2 (25 ng/ml) plus Noggin (50 ng/ml) and Surfen (5 μM) plus Noggin (50 ng/ml) in 0.1%BSA/DMEM for 15 min, 30 min, 1 h, 2 h and 6 h. Doses used were based on previous studies (18,67). Cultures were lysed in 1X RIPA with protease and phosphatase inhibitors, and samples were centrifuged at 13,200 rpm at 4°C and supernatants were collected. Protein concentration for each sample was determined using the MicroBCA Protein Assay Kit (Thermo Scientific) according to the manufacturer's protocol. Total cellular proteins (30 μg/lane) were electrophoresed on 4-12% NuPAGE Bis-Tris gels (Life Technologies) and transferred to PVDF membranes (Millipore). Membranes were blocked in 5% BSA/1X Tris Buffered Saline/Tween 20 (TBST) and incubated overnight at 4°C with phosphoSMAD1/5/8 (pSMAD1/5/8) (1:1000; Cell Signaling). Membranes were washed in 1X TBST and incubated with anti-rabbit HRP-linked antibody (1:2000; Cell Signaling) for 1 hr at room temperature. Antigen-antibody complexes were detected with SuperSignal® West Dura Extended Duration Substrate (Thermo Scientific) chemiluminescent detection system using the ImageQuant LAS 4000 luminescent image analyzer (GE Healthcare). Membranes were re-blotted with SMAD1 (1:1000; Cell Signaling) for normalization. For loading control, membranes were blotted with GAPDH antibodies (1:1000; Santa Cruz Biotechnology). To detect the mature form of BMP2, membranes were blocked in 5% nonfat dried milk/1X TBST and incubated overnight at 4°C with anti-BMP2 (1:1000; Abcam) and GAPDH (1:1000; Santa Cruz Biotechnology). After washing, the membranes were incubated with secondary antibodies, anti-rabbit HRP-linked antibody and anti-mouse HRP-linked antibody. Primary and secondary antibodies were diluted in 5% nonfat dried milk/1X TBST. Antigen-antibody complexes were detected as mentioned above. ImageJ was used to determine band intensities.

Gene Expression Analysis - Total RNA was isolated from control, rhBMP2-treated, Surfen-treated, Noggin-treated, rhBMP2 plus Noggin-treated and Surfen plus Noggin-treated transfected or non-transfected Ad-293 and C3H/10T/1/2 cultured cells from 6 well plates (67), using TRIzol reagent (cat# 15596-026, Life Technologies) according to the manufacturer's protocol. RNA was quantified by Nanodrop. One microgram total RNA was reversed transcribed using the Verso cDNA kit (cat# AB1435/A, Thermo Scientific). Quantitative real-time PCR was carried out using SYBR Green PCR Master Mix (Applied Biosystems) in an Applied Biosystems 7500 machine according to manufacturer's protocol. *Gapdh* was used as the endogenous control and relative expression was calculated using the ΔΔCT method. Real-time PCRwas performed using GoTaq DNA Polymerase (Promega) in a ProFlex PCR System (Applied Biosystems) for 30 cycles. PCR products were resolved on a 2% agarose gel. Primer sequences for all PCR primers can be found in Supplemental Table 2.

Fluorescence-activated cell sorting (FACS) – Ad-293 cells were grown in DMEM containing 10% FBS in 6 well plates. The cells were treated with DMSO or Surfen (5 μM) for 1 hr at 37°C in DMEM containing 0.1% BSA. Following treatment, the cells were washed with 1X PBS and removed from the plates by scraping in 1X PBS, 2 mM EDTA or by trypsin. The cells were washed with 1X PBS and fixed with 2% buffered formalin for 15 min on ice. The cells were washed with 1X PBS and blocked by incubation in 1X PBS/1% BSA (PBSB) for 10 min on ice. Aliquots of 10^6 cells (100 μl) were

incubated with control mouse IgG (Cell Signaling # 5415) or anti-BMP-2/4 Antibody (H-1; Santa Cruz) in 1X PBSB on ice for 2 h. The cells were washed and incubated with an Alexa 488 Goat Anti-Mouse IgG (Jackson Immuno-Research) for 1 h on ice. The cells were washed with 1X PBS and analyzed on a BD Accuri flow cytometer, located in the Flow Cytometry Core Laboratory at CHOP. The data was analyzed using CFlow Plus software. The Accuri C6 recorded 10,000 events then the Ad-293 cell population. The established gate was used in subsequent readings (10,000 events) and the mean FL1-A values of the gated cells were graphed.

Fluorescence Recovery After Photobleaching (FRAP)- Ad-293 cells were grown in 35 mm glass bottom well dishes coated with poly-d-lysine (MatTek) and transfected with 1 μg per 35 mm dish of *Snap-BMPRIa* or *Snap-BMPRII* for 24 h using Fugene 6 transfection reagent. After 24 h the cells were incubated with 2 μM of SNAP-tag 488 (New England Biolabs) for 30 minutes at 37°C. Cells were then washed three times with complete media and imaged in FluoroBrite™ DMEM media (ThermoFisher Scientific). Cells were stimulated with vehicle (1X PBS or DMSO), rhBMP2 (50 ng/ml), Surfen (5 μM), Noggin (50 ng/ml), rhBMP2 plus Noggin or Surfen plus Noggin. FRAP was performed on a laser scanning confocal microscope (Olympus FV-1000) with an IX81 inverted microscope equipped with dual scanners for simultaneous imaging and stimulation bleaching. A 40X oil immersion objective lens with an aperture of 1.30 (Olympus UPlanFL) was used for imaging. Additionally, we used an Argon ion laser and HeNe laser for imaging and a 405 diode laser for bleaching under the control of Fluoview software. 35 mm glass bottom well dishes were placed in a circular holder connected to a heating system so that all FRAP assays were carried out at 37°C. A small circular region of the membrane was bleached for 200 ms at 50% laser power. Images were taken approximately every 3 seconds over a period of 250 seconds. A series of 15 pre-bleached images were taken, followed by the bleaching and recovery. The images were analyzed by Fiji (ImageJ) and corrected and normalized by FRAP Analyzer software. The normalized values were plotted nonlinear regression curve fit and one-phase association (Graph Pad Prism 6) to calculate the halftime recovery ($\tau_{1/2}$) and mobile fraction (F_m).

Detergent Resistant Membrane (DRM) Isolation - Ad-293 cells were grown in 100 mm dishes and transfected with 8 μg of *Snap-BMPRIa* or *Snap-BMPRII* plasmid and 18 μl of Fugene 6 reagent per 100 mm dish. After 48 h cells were treated with vehicle (1X PBS or DMSO) or Surfen (5 μM) for 10 minutes at 37°C. DRM isolation was carried out according to previous studies (44,45). Briefly, cells were washed with ice-cold 1X PBS and ice-cold 1X Tris-HCl, NaCl and EDTA (TNE). Lysates were collected in 1X TNE and centrifuged for 5 min at 380 g at 4°C. The pellets were resuspended in 275 μl of 1X TNE plus protease inhibitors and homogenized via a 25-gauge needle. Following homogenization, 250 μl of 2% Triton X-100 was added to 250 μl of the cell homogenate and placed on ice for 30 minutes. For the step sucrose gradient, 1.25 ml of 56% sucrose was added to the sample for a final percentage of 40% sucrose. The solution was transferred to a 5 ml centrifuge tube (Beckman Coulter). The sample was overlayed with 2.75 ml of 35% sucrose and then 0.25 ml of 5% sucrose. The samples were centrifuged for 18 h at 39,000 rpm at 4°C using an SW55 Ti rotor. The next day, 15 fractions of 300 μl each were collected per condition. The samples were electrophoresed on 4-12% NuPAGE Bis-Tris gels and transferred to PVDF membranes. Membranes were blocked in 5% BSA/1X Tris Buffered Saline/Tween 20 (TBST) and incubated overnight at 4°C with anti-SNAP-tag (1:1000; New England Biolabs) and caveolin-1 (1:1000; Cell Signaling). Membranes were washed in 1X TBST and incubated with anti-rabbit HRP-linked antibody (1:2000; Cell Signaling) for 1 hr at room temperature. Antigen-antibody complexes were detected with SuperSignal® West Dura Extended Duration Substrate chemiluminescent detection system.

Proximity Ligation Assay (PLA) – This procedure was carried out based on established

methods (47,48). Ad-293 cells and C2H/10T1/2 cells were grown on poly-L-lysine coated coverslips in 12-well plates. Cells were treated with vehicle (1X PBS/DMSO), rhBMP2 (50 ng/ml), or Surfen (5 μM) for 10 minutes at 37°C. For Noggin experiments, rhBMP2 (25 ng/ml) or Surfen (5 μM) were preincubated with Noggin (50 ng/ml) for 10 minutes at 37°C before addition to the cell culture media. Cells were then washed with 1X PBS and fixed in 2% PFA. After fixation cells were rinsed in 1X PBS and blocked in 1% BSA/1X PBS for 30 minutes at room temperature. Cells were incubated with the following antibodies overnight at 4°C: rabbit anti-BMPRIa (1:75; Origene) and mouse anti-BMPRII (1:250; Thermo Fisher Scientific). mouse IgG (Cell Signaling) and rabbit IgG (Cell Signaling) were used for negative controls. The next day, we performed Duolink In situ Red Starter PLA Kit Mouse/Rabbit (Sigma) according to the manufacturer's protocol. Briefly, the cells were washed with 1X PBS and incubated with anti- rabbit plus probe and anti-mouse minus probe solution for 1 h at 37°C. Next, cells were incubated in ligation solution for 30 minutes at 37°C. Following ligation, the signal was amplified via polymerase by incubating the cells in amplification solution for 100 minutes at 37°C. Cells were washed with wash buffer and allowed to dry for 10 minutes in the dark. Coverslips were inverted and mounted onto glass slides using Duolink In Situ Mounting Medium with DAPI. Slides were imaged on a Nikon Eclipse TE2000-U microscope using a 20X/0.75 objective and a 40X/0.95 dry objective (Nikon Plan Apo). Images were captured using an Evolution QEi monochrome camera (Media Cybernetics) and NIS Elements BR 3.2 software. Color was added to images and blue and red channels were merged through the ImageJ program. To quantify the fluorescent red amplification dots/cell, images were made binary under an RGB threshold and "Particle Analysis" was utlilized through Image J.

Statistical Analysis - Results were analyzed using GraphPad Prism 6 software. A one-way Analysis of Variance (ANOVA) with a Tukey's Multiple Comparison Test or Student's T-test was used to identify the differences. Threshold for significance for all tests was set as $p < 0.05$.

ACKNOWLEDGMENTS: The study was supported by the NIAMS grants R01AR061758 and AR071946 to MP. We acknowledge the passionate efforts of the Multiple Hereditary Exostoses Research Foundation (www.mherf.org), an private non-profit organization dedicated to the support of patients with MHE and their families and advocating MHE public awareness and biomedical research. We would like to also acknowledge Christopher's Cure (www.facebook.com/christopherscure) created by the Muth's family, an organization devoted to conquering rare childhood cancer.

CONFLICT OF INTEREST: The authors declare that they have no conflicts of interest with the contents of this article.

AUTHOR CONTRIBUTIONS: C.M. and M.P. designed the experiments. C.M. performed most of the experiments. P.B. and E.Y designed and performed FACS analyses. H.T. provided technical expertise in conducting FRAP assays and data interpretation and assisted in manuscript revision. C.M., P.B. and M.P analyzed the data. C.M and M.P wrote and revised the manuscript.

REFERENCES

1. Luckert Wicklund, C. L., Pauli, R. M., Johnson, D. R., and Hecht, J. T. (1995) Natural history of Hereditary Multiple Exostoses. *Am. J. Med. Genet.* **55**, 43-46

2. Schmale, G. A., Conrad, E. U., and Raskind, W. H. (1994) The natural history of hereditary multiple exostoses. *J. Bone Joint Surg. Am.* **76**, 986-992

3. Sinha, R., Mundy, C., Bechtold, T., Sgariglia, F., Ibrahim, M. M., Billings, P. C., Carroll, K., Koyama, E., Jones, K. B., and Pacifici, M. (2017) Unsuspected osteochondroma-like outgrowths in the cranial base of Hereditary Multiple Exostoses patients and modeling and treatment with a BMP antagonist in mice. *PLoS Genetics* **13**, e1006742

4. Solomon, L. (1963) Hereditary multiple exostosis. *J. Bone Joint Surg.* **45B**, 292-304

5. Dormans, J. P. (2005) *Pediatric Orthopaedics: Core Knowledge in Orthopaedics*, Elsevier Mosby, Philadelphia

6. Uchida, K., Kurihara, Y., Sekiguchi, S., Doi, Y., Matsuda, K., Miyanaga, M., and Ikeda, Y. (1997) Spontaneous haemothorax caused by costal exostosis. *Eur. Respir. J.* **10**, 735-736

7. Ahn, J., Ludecke, H. J., Lindow, S., Horton, W. A., Lee, B., Wagner, M. J., Horsthemke, B., and Wells, D. E. (1995) Cloning of the putative tumour suppressor gene for hereditary multiple exostoses (EXT1). *Nat. Genet.* **11**, 137-143

8. Cheung, P. K., McCormick, C., Crawford, B. E., Esko, J. D., Tufaro, F., and Duncan, G. (2001) Etiological point mutations in the hereditary multiple exostoses gene EXT1: a functional analysis of heparan sulfate polymerase activity. *Am. J. Hum. Genet.* **69**, 55-66

9. Hecht, J. T., Hogue, D., Strong, L. C., Hansen, M. F., Blanton, S. H., and Wagner, H. (1995) Hereditary multiple exostosis and chondrosarcoma: linkage to chromosome 11 and loss of heterozygosity for EXT-linked markers on chromosome 11 and 8. *Am. J. Hum. Genet.* **56**, 1125-1131

10. Wuyts, W., and Van Hul, W. (2000) Molecular basis of multiple exostoses: mutations in the EXT1 and EXT2 genes. *Hum. Mutat.* **15**, 220-227

11. Anower-E-Khuda, M. F., Matsumoto, K., Habuchi, H., Morita, H., Yokochi, T., Shimizu, K., and Kimata, K. (2013) Glycosaminoglycans in the blood of hereditary multiple exostoses patients: half reduction of heparan sulfate to chondroitin sulfate ratio and the possible diagnostic application. *Glycobiology* **23**, 865-876

12. McCormick, C., Duncan, G., Goutsos, K. T., and Tufaro, F. (2000) The putative tumor suppressors EXT1 and EXT2 form a stable complex that accumulates in the Golgi complex and catalyzes the synthesis of heparan sulfate. *Proc. Natl. Acad. Sci. USA* **97**, 668-673

13. Huegel, J., Sgariglia, F., Enomoto-Iwamoto, M., Koyama, E., Dormans, J. P., and Pacifici, M. (2013) Heparan sulfate in skeletal development, growth, and pathology: the case of Hereditary Multiple Exostoses. *Dev. Dyn.* **242**, 1021-1032

14. Billings, P. C., and Pacifici, M. (2015) Interactions of signaling proteins, growth factors and other proteins with heparan sulfate: mechanisms and mysteries. *Connect. Tissue Res.* **56**, 272-280

15. Bishop, J. R., Schuksz, M., and Esko, J. D. (2007) Heparan sulphate proteoglycans fine-tune mammalian physiology. *Nature* **446**, 1030-1037

16. Lin, X. (2004) Functions of heparan sulfate proteoglycans in cell signaling during development. *Development* **131**, 6009-6021

17. Xu, D., and Esko, J. D. (2014) Demystifying heparan sulfate-protein interactions. *Annu. Rev. Biochem.* **83**, 129-157

18. Huegel, J., Mundy, C., Sgariglia, F., Nygren, P., Billings, P. C., Yamaguchi, Y., Koyama, E., and Pacifici, M. (2013) Perichondrium phenotype and border function are regulated by Ext1 and heparan sulfate in developing long bones: A mechanism likely deranged in Hereditary Multiple Exostoses. *Dev. Biol.* **377**, 100-112

19. Inubushi, T., Nazawa, S., Matsumoto, K., Irie, F., and Yamaguchi, Y. (2017) Aberrant perichondrial BMP signaling mediates multiple osteochondromagenesis in mice. *J. Clin. Inv. Insight* **2**, e90049

20. Gilboa, L., Nohe, A., Geissendorfer, T., Sebald, W., Henis, Y. I., and Knaus, P. (2000) Bone morphogenetic protein receptor complexes on the surface of live cells: a new oligomerization mode for serine/threonine kinase receptors. *Mol. Biol. Cell* **11**, 1023-1035

21. Greenwald, J., Groppe, J., Gray, P., Wiater, E., Kwiatkowski, W., Vale, W., and Choe, S. (2003) The BMP7/AchRII extracellulaer domain complex provides new insights into the cooperative natue of receptor assembly. *Mol. Cell* **11**, 605-617

22. Groppe, J., Hinck, C. S., Samavarchi-Tehrani, P., Zubieta, C., Schuermann, J. P., Taylor, A. B., Schwarz, P. M., Wrana, J. L., and Hinck, A. P. (2008) Cooperative assembly of TGF-beta superfamily signaling complexes is mediated by two disparate mechanisms and distinct modes of receptor binding. *Mol. Cell* **29**, 157-168

23. Salazar, V. S., Gamer, L. W., and Rosen, V. (2016) BMP signaling in skeletal development, disease and repair. *Nat. Rev. Endocrinology* **12**, 203-221

24. Erlich, M., Gutman, O., Knaus, P., and Henis, Y. I. (2012) Oligomeric interactions of TFG-β and BMP receptors. *FEBS Lett.* **586**, 1885-1896

25. Guzman, A., Zelman-Femiak, M., Boergermann, J. H., Pashkowsky, S., Kreuzaler, P. A., Fratzl, P., Harns, G. S., and Knaus, P. (2012) SMAD versus non-SMAD signaling is determined by lateral mobility of bone morphogenetic protein (BMP) receptors. *J. Biol. Chem.* **287**, 39492-39504

26. Hartung, A., Bitton-Worms, K., Rechtman, M. M., Wenzel, V., Boergermann, J. H., Hassel, S., Henis, Y. I., and Knaus, P. (2006) Different routes of bone morphogenetic protein (BMP) receptor endocytosis influence BMP signaling. *Mol. Cell Biol.* **26**, 7791-7805

27. Marom, B., Heining, E., Knaus, P., and Henis, Y. I. (2011) Formation of stable homomeric and transient heteromeric bone morphogenetic protein (bmp) receptor complexes regulates smad protein signaling. *J. Biol. Chem.* **286**, 19287-19296

28. Massague, J. (2012) TGFβ signaling in context. *Nat. Rev. Mol. Cell. Biol.* **13**, 616-630

29. Balemans, W., and Van Hul, W. (2002) Extracellular regulation of BMP signaling in vertebrates: a cocktail of modulators. *Dev. Biol.* **250**, 231-250

30. Weiss, A., and Attisano, L. (2013) The TGFbeta superfamily signaling pathway. *WIREs Dev. Biol.* **2**, 47-63

31. Kuo, W.-J., Digman, M. A., and Lander, A. D. (2010) Heparan sulfate acts as a bone morphogenetic protein co-receptor by facilitating ligand-induced receptor hetero-oligodimerization. *Mol. Biol. Cell* **21**, 4028-4041

32. Jiao, X., Billings, P. C., O'Connell, M. P., Kaplan, F. S., Shore, E., and Glaser, D. L. (2007) Heparan sulfate proteoglycans (HSPGs) modulate BMP2 osteogenic bioactivity in C2C12 cells. *J. Biol. Chem.* **282**, 1080-1086

33. Manton, K. J., D.F.M., L., Cool, S. M., and Nurcombe, v. (2007) Disruption of heparan and chondroitin sulfate signaling enhances mesenchymal stem cell-derived osteogenic differentiation via bone morphogenetic protein signaling pathways. *Stem Cells* **25**, 2845-2854

34. Huegel, J., Enomoto-Iwamoto, M., Sgariglia, F., Koyama, E., and Pacifici, M. (2015) Heparanase stimulates chondrogenesis and is up-regulated in human ectopic cartilage. A mechanism possibly involved in Hereditary Multiple Exostoses. *Am. J. Path.* **185**, 1676-1685

35. Ohkawara, B., Iemura, S., ten Dijke, P., and Ueno, N. (2002) Action range of BMP is defined by its N-terminal basic amino acid core. *Curr. Biol.* **12**, 205-209

36. Ruppert, R., Hoffmann, E., and Sebald, W. (1996) Human bone morphogenetic protein 2 contains a heparin-binding site which modifies its biological activity. *Eur. J. Biochem.* **237**, 295-302

37. Haas, A. R., and Tuan, R. S. (1999) Chondrogenic differentiation of murine C3HT1/2 multipotential mesenchymal cells: II. Simulation by bone morphogenetic protein-2 requires modulation of N-cadherin expression and function. *Differentiation* **64**, 77-89

38. Hatsell, S. J., Idone, V., Alessi Wolken, D. M., Huang, L., Kim, H. J., Wang, L. C., Wen, X., Nannuru, K. C., Jimenez, J., Xie, L., das, N., Makhoul, G., Chernomorsky, R., D'Ambrosio, D., Corpina, R. A., Schoenherr, C. J., Feeley, K., Yu, P. B., Yancopoulos, G. D., Murphy, A. J., and Economides, A. N. (2015) ACVR1R206H receptor mutation causes fibrodysplasia ossificans progressiva by imparting responsiveness to activin A. *Science Trans. Med.* **7**, 303ra137

39. Schuksz, M., Fuster, M. M., Brown, J. R., Crawford, B. E., Ditto, D. P., Lawrence, R., Glass, C. A., Wang, L. C., Tor, Y., and Esko, J. D. (2008) Surfen, a small molecule antagonist of heparan sulfate. *Proc. Natl. Acad. Sci. USA* **105**, 13075-13080

40. Brunet, L. J., McMahon, J. A., McMahon, A. P., and Harland, R. M. (1998) Noggin, cartilage morphogenesis, and joint formation in the mammalian skeleton. *Science* **280**, 1455-1457

41. Simons, K., and Toomre, D. (2000) Lipid rafts and signal transduction. *Nat. Rev. Mol. Cell Biol.* **1**, 31-39

42. Doumazane, E., Scholler, P., Zwier, J. M., Trinquet, E., Rondart, P., and Pin, J. P. (2011) A new approach to analyze cell surface protein complexes reveals specific heterodimeric metabotropic glutamate receptors. *FASEB J.* **25**, 66-77

43. Gautier, A., Juillerat, A., Heinis, C., Correa, I. R., Kindermann, M., Beaufils, F., and Johnsson, K. (2008) An engineered protein tag for multiprotein labeling in living cells. *Chem. Biol.* **15**, 128-136

44. Brown, D. A., and London, E. (2000) Structure and function of sphingolipid- and cholesterol-rich membrane rafts. *J. Biol. Chem.* **275**, 17221-17224

45. Sargiacomo, M., Sudol, M., Tang, Z., and Lisanti, M. P. (1993) Signal transduction molecules and glycosyl-phosphatidylinositol-linked proteins form a celeolin-rich insoluble complex in MDCK cells. *J. Cell Biol.* **122**, 789-807

46. Anderson, R. G., and Jacobson, K. (2002) A role of lipid shells in targeting proteins to caveolae, rafts, and othe rlipid domains. *Science* **296**, 1821-1825

47. Soderberg, O., Gullberg, M., Jarvius, M., Riidderstrale, K., Leuchowius, K.-J., Jarvius, J., Wester, K., Hydbring, P., Bahram, F., Larsson, L., and Landergren, U. (2006) Direct observation of individual endogenous protein complexes in situ by proximity ligation. *Nat. Methods* **3**, 995-1000

48. Bellucci, A., Fiorentini, C., Zaltieri, M., Missale, C., and Spano, P. (2014) The "in situ" proximity ligation assay to probe protein-protein interactions in intact tissues. *Methods Mol. Biol.* **1174**, 397-405

49. Kholodenko, B. N. (2006) Cell signaling dynamics in time and space. *Nat. Rev. Mol. Cell Biol.* **7**, 165-176

50. Thomas, P., and Smart, T. G. (2006) Receptor dynamics at the cell surface studied using functional tagging. in *The Dynamic Synapse; Molecular Methods in Ionotropic Receptor*

Biology. (Kittler, J. T., and Moss, S. J. eds.), CRC Press/Talyor $ Francis, Boca Raton, FL. pp

51. Beauvais, D. M., Burbach, B. J., and Rapraeger, A. C. (2004) The syndecan-1 ectodomain regulates alpha (v) beta 3 integrin activity in mammalaina carcinoma cells. *J. Cell Biol.* **167**, 171-181

52. Whiteford, J. R., Xian, X., Chaussade, C., Vanhaesebroeck, B., Nourshargh, S., and Couchman, J. R. (2011) Syndecan-2 is a novel ligand for the protein tyrosine phosphatase receptor CD148. *Mol. Biol. Cell* **22**, 3609-3624

53. Brown, A., Robinson, C. J., Gallagher, J. T., and Blundell, T. L. (2013) Cooperative heparin-mediated oligomerization of fibroblast growth factors (FGF1) precedes recruitment of FGFR2 to ternary complexes. *Biophys. J.* **104**, 1720-1730

54. Ibrahimi, O. A., Zhang, F., Hrstka, S. C., Mohammadi, M., and Linhardt, R. J. (2004) Kinetic model of FGF, FGFR, and proteoglycan signal transduction complex assembly. *Biochemistry* **43**, 4724-4730

55. Pohl, T. L. M., Boergermann, J. H., Schwaerzer, G. K., Knaus, P., and Cavalcanti-Adam, E. A. (2012) Surface immobilization of bone morphogenetic protein 2 via a self-assembled monolayer formation induces cell differentiation. *Acta Biomaterialia* **8**, 772-780

56. Chen, S., Wassenhove-McCarthy, D. J., Yamaguchi, Y., Holzman, B., van Kuppevelt, T. h., Jenniskens, G., Wijnhoven, T. J., Woods, A. C., and McCarthy, K. J. (2008) Loss of heparan sulfate glycosaminoglycan assembly in podocytes does not lead to proteinuria. *Kidney Int.* **74**, 289-299

57. Mooij, H. L., BernelotMoens, S. J., Gordts, P. L., Stanford, K. I., Foley, E. M., van den Boogert, M. A., Witjes, J. J., Hassig, H. C., Tanck, M. W., van de Sande, M. A., Levels, J. H., Kstelein, J. J., Stroes, E. S., Dallinga-Thie, G. M., Esko, J. D., and Nieuwdorp, M. (2015) Ext1 heterozygosity causes a modest effect on postprandial lipid clearance in humans. *J. Lipid Res.* **56**, 665-673

58. Knudson, A. G. (1996) Hereditary cancer: two hits revisited. *J. Cancer Res. Clin. Oncol.* **122**, 135-140

59. Jones, K. B., Piombo, V., Searby, C., Kurriger, G., Yang, B., Grabellus, F., Roughley, P. J., Morcuende, J. A., Buckwalter, J. A., Capechhi, M. R., A., V., and Sheffield, V. C.

(2010) A mouse model of osteochondromagenesis from clonal inactivation of Ext1 in chondrocytes. *Proc. Natl. Acad. Sci. USA* **107**, 2054-2059

60. Matsumoto, K., Irie, F., Mackem, S., and Yamaguchi, Y. (2010) A mouse model of chondrocyte-specific somatic mutation reveals a role for Ext1 loss of heterozygosity in multiple hereditary exostoses. *Proc. Natl. Acad. Sci. USA* **107**, 10932-10937

61. Sgariglia, F., Candela, M. E., Huegel, J., Jacenko, O., Koyama, E., Yamaguchi, Y., Pacifici, M., and Enomoto-Iwamoto, M. (2013) Epiphyseal abnormalities, trabecular bone loss and articular chondrocyte hypertrophy develop in the long bones of postnatal Ext1-deficient mice. *Bone* **57**, 220-231

62. Zak, B. M., Schuksz, M., Koyama, E., Mundy, C., Wells, D. E., Yamaguchi, Y., Pacifici, M., and Esko, J. D. (2011) Compound heterozygous loss of Ext1 and Ext2 is sufficient for formation of multiple exostoses in mouse ribs and long bones. *Bone* **48**, 979-987

63. Bandyopadhyay, A., Kubilus, J. K., Crochiere, M. L., Linsenmayer, T. F., and Tabin, C. J. (2008) Identification of unique molecular subdomains in the perichondrium and periosteum and their role in regulating gene expression in the underlying chondrocytes. *Dev. Biol.* **321**, 162-174

64. Hojo, H., Ohba, S., Taniguchi, K., Shirai, M., Yano, F., Saito, T., Ikeda, T., Nakajima, K., Komiyama, Y., Nakagata, N., Suzuki, K., Mishina, Y., Yamada, M., Konno, T., Takato, T., Kawaguchi, H., Kambara, H., and Chung, U.-I. (2013) Hedgehog-Gli activators direct osteo-chondrogenic function in bone morphogenetic protein toward osteogenesis in the perichondrium. *J. Biol. Chem.* **288**, 9924-9932

65. Minina, E., Schneider, L., Rosowski, M., Lauster, R., and Vortkamp, A. (2005) Expression of Fgf and Tgfbeta signaling related genes during embryonic endochondral ossification. *Gene Exp. Patterns* **6**, 102-109

66. Matsushita, T., Chan, Y. Y., Kawanami, A., Balmes, G., Landreth, G. E., and Murakami, S. (2009) Extracellular signal-regulated kinase 1 (ERK1) and ERK2 play essential roles in osteoblast differentiation and in supporting osteoclastogenesis. *Mol. Cell. Biol.* **29**, 5843-5857

67. Mundy, C., Bello, A., Sgariglia, F., Koyama, E., and Pacifici, M. (2016) HhAntag, a hedgehog signaling antagonist, suppresses chondrogenesis and modulates canonical and non-canonical BMP signaling. *J. Cell. Physiol.* **231**, 1033-1044

Figure 1. HS interference stimulates BMP signaling in Ad-293 cells and C3H/10T1/2 cells. *A* and *B*, scatterplots of qPCR data showing that treatment of Ad-293 cells and C3H/10T1/2 cells with rhBMP2 (25 ng/ml) or Surfen (5 μM) caused a significant increase in *Id1* compared to vehicle-treated cells. *C and D*, representative immunoblot images revealing that treatment with rhBMP2 or Surfen caused an increase in pSMAD 1/5/8 protein levels in Ad-293 cells relative to control. *E and F,* immunoblot images revealing that rhBMP2 (25 ng/ml in 0.1%BSA/DMEM) or Surfen (5 μM in 0.1%BSA/DMEM) treatment elicited maximal pSMAD1/5/8 protein levels at 1 and 6 h, respectively. *G-J,* quantification of pSMAD 1/5/8 / SMAD 1 levels in BMP2 and Surfen-treated cell lysates. (* $p < 0.05$; ** $p < 0.01$; *** $p < 0.001$; **** $p < 0.0001$). Results were analyzed using one-way ANOVA with Tukey's multiple comparisons tests and are expressed as mean ± S.D. for n = 3 separate experiments.

Figure 2. Endogenous mature BMPs are present at the cell surface. *A-E,* FACS plots depicting fluorescent intensity (horizontal axis) against counts (vertical axis). *A and B*, control cells exposed to no primary (1°) and 2° antibodies or 2° antibody only produced fluorescent peaks around 10^3 and 10^4, respectively. *D and E,* vehicle- and Surfen-treated cells exposed to BMP2/4 antibody plus 2° antibody produced a fluorescent peak between 10^5 and 10^6, which was much higher than that produced by cells exposed to preimmune 1° plus 2° antibody (*C)*. *F,* quantification of relative fluorescence values in each depicted intensity plot. Note that pre-treatment with trypsin drastically reduced fluorescent levels. *G,* immunoblots depicting levels of mature form of BMP2 in control and Surfen-treated cells. Five, 15 and 30 μg of whole cell proteins were loaded per lane. *H,* quantification of relative BMP2 protein levels after GAPDH normalization. Results were analyzed using Student's T-test and are expressed as mean ± S.D. for n = 3 separate experiments.

Figure 3. Snap-BMPRIa and Snap-BMPRII localize to the cell surface and activate BMP signaling in Ad-293 cells. *A and C,* uniform localization of Snap-BMPRIa and Snap-BMPRII along the cell surface membrane of Ad-293 cells, with minimal detectable intracellular accumulation. *B,* scatterplot of qPCR data showing that treatment with rhBMP2 (25 ng/ml) or Surfen (5 μM) of co-transfected cells caused a significant up-regulation in BMP early response gene *Id1* expression compared to companion vehicle-treated cells**.** *D and E*, representative immunoblot images and quantification showing that rhBMP2 or Surfen treatment significantly increased pSMAD 1/5/8 protein levels relative to untreated cells. (* $p < 0.05$; ** $p < 0.01$; **** $p < 0.0001$). Results were analyzed using one-way ANOVA with Tukey's multiple comparisons tests and are expressed as mean ± S.D. for n = 3 separate experiments.

Figure 4. HS interference causes a reduction in BMPRII surface mobility. *A,* representative Snap-BMPRII expressing Ad-293 cell in which a region of interest was identified and is depicted by a yellow box. *B-E,* magnified images of the region of interest show pre-bleach at 0 s, bleach at 50 s and recovery at 130 s and 215 s. *F-H,* fluorescence intensity quantification of photobleached areas and calculated half time recovery ($\tau 1/2$) and mobile fraction (F_m). Treatment with rhBMP2 or Surfen caused a significant increase in $\tau 1/2$ (*G-I*) and a decrease in the F_m population (*J*) compared to control Snap-BMPRII expressing Ad- 293 cells. (** $p < 0.01$; **** $p < 0.0001$) Results were analyzed using one-way ANOVA with Tukey's multiple comparisons tests and are expressed as mean ± S.D. for n = 17-30 cells per condition.

Figure 5. HS interference does not significantly alter BMPRIa surface mobility. *A,* representative Snap-BMPRIa expressing Ad-293 cell in which a region of interest was identified and is depicted by a yellow box. *B-E,* magnified images of the region of interest show pre-bleach at 0 s, bleach at 50 s and recovery at 130 s and 215 s. *F-H,* fluorescence intensity quantification of photobleached area and calculated half time recovery ($\tau 1/2$) and mobile fraction (F_m). Treatment with rhBMP-2 or Surfen caused no major difference in $\tau 1/2$ (*G-I*) or F_m (*J*) when compared to control Snap-BMPRIa expressing 293 cells.

Results were analyzed using one-way ANOVA with Tukey's multiple comparisons tests and are expressed as mean ± S.D. for n = 17-30 cells per condition.

Figure 6. Surfen promotes recruitment of BMPRII population to lipid raft domains. vehicle-treated (*A and B)* and Surfen-treated Ad-293 cells (*C and D)* expressing Snap-BMPRII or Snap-BMPRIa were homogenized and fractionated by sucrose gradient ultracentrifugation. Fractions were blotted with anti-Snap or anti-caveolin 1 antibodies. *A,* in vehicle-treated cells, the BMPRII population is distributed in both lipid raft and non-lipid raft domains. *C,* in Surfen-treated cells, there is a robust shift in BMPRII population to lipid raft domains, depicted in particular in fraction 1. *B,* in vehicle-treated cells, the BMPRIa population is mostly in the lipid raft domains. *D,* in Surfen-treated cells, the majority of the BMPRIa population is seen in lipid raft domains, but there is a significant amount of receptors in the non-lipid raft domains compared to the control cells. *E* and *F,* Quantification of receptor population in either DRM or non-DRM. (* $p < 0.05$). Results were analyzed using Student's T-test and are expressed as mean ± S.D. for n = 3 separate experiments.

Figure 7. HS interference leads to increased BMPRIa and BMPRII interactions. Antibody-based in situ proximity ligation assays were used to analyze BMPRIa and BMPRII interactions in Ad-293 and C3H10T1/2 cells. Treatment with rhBMP2 (25 ng/ml) or Surfen (5 μM) led to a striking increase in receptor-receptor interactions (depicted by red fluorescence dots) in both Ad-293 cells (*B, C, F and G*) and C3H/10T1/2 cells (*J, K, N and O*) compared to control cells (*A, E, I and M*). Companion cells reacted with preimmune antibodies exhibited no signal (*D, H, L and P*), attesting to specificity of analysis. Note that *E-H* and *M-P* are magnified images of representative fields from each culture shown in *A-D* and *I-L*. Scale bar: 50 μm. *Q and R,* scatterplots depicting quantification of fluorescent signal per cell in each condition. (** $p < 0.01$; *** $p < 0.001$; **** $p < 0.0001$). Results were analyzed using one-way ANOVA with Tukey's multiple comparisons tests and are expressed as mean ± S.D. for n = 17-30 cells per condition.

Figure 8. Schematic depicting distribution of BMPRs and HSPGs prior or after treatment with rhBMP2 or Surfen. *A,* in control cells, the BMPRIa population would be located predominantly in lipid raft domains (orange membrane section), whereas the BMPRII population would be more widely distributed over non-lipid raft domains. Endogenous BMPs would largely be bound to HS and limit interactions with BMPRs and signaling. *B,* treatment with rhBMP2 would cause a major and rapid redistribution of BMPRIIs to lipid rafts, interactions with resident BMPRIa population and strong downstream signaling. Excess rhBMP2 would accumulate onto HSPGs. *C,* in Surfen-treated cells, the drug would compete with HS-BMP binding, promote availability and engagement of endogenous BMPs, and stimulate BMPRII recruitment to lipid rafts, interactions with BMPRIa and downstream signaling.

Figure 1

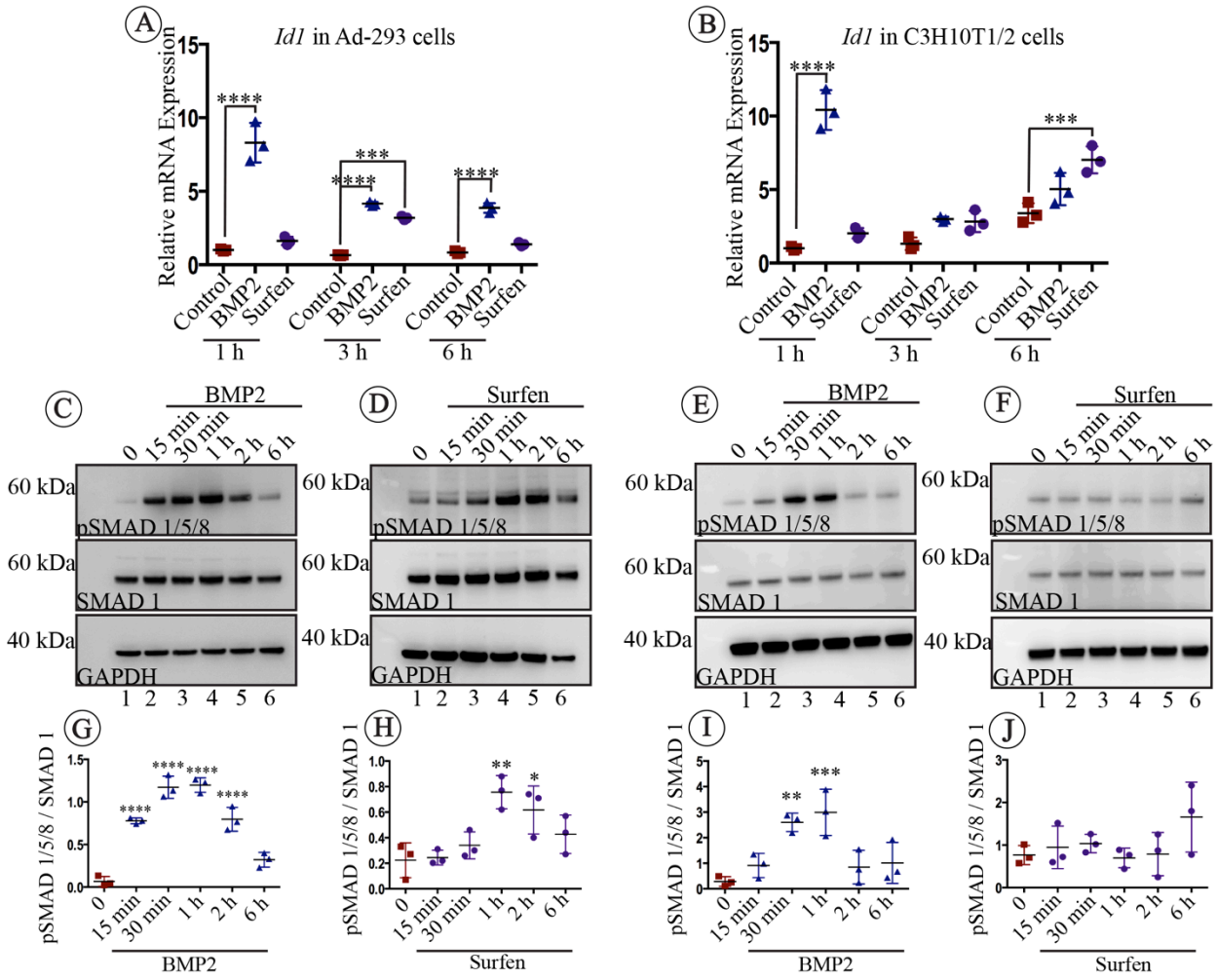
A
Id1 in Ad-293 cells
Relative mRNA Expression
Control
BMP2
Surfen
1 h
3 h
6 h
B
Id1 in C3H10T1/2 cells
C
BMP2
D
Surfen
0 15 min 30 min 1 h 2 h 6 h
60 kDa
pSMAD 1/5/8
SMAD 1
40 kDa
GAPDH
1 2 3 4 5 6
E
F
G
pSMAD 1/5/8 / SMAD 1
H
I
J

Figure 2

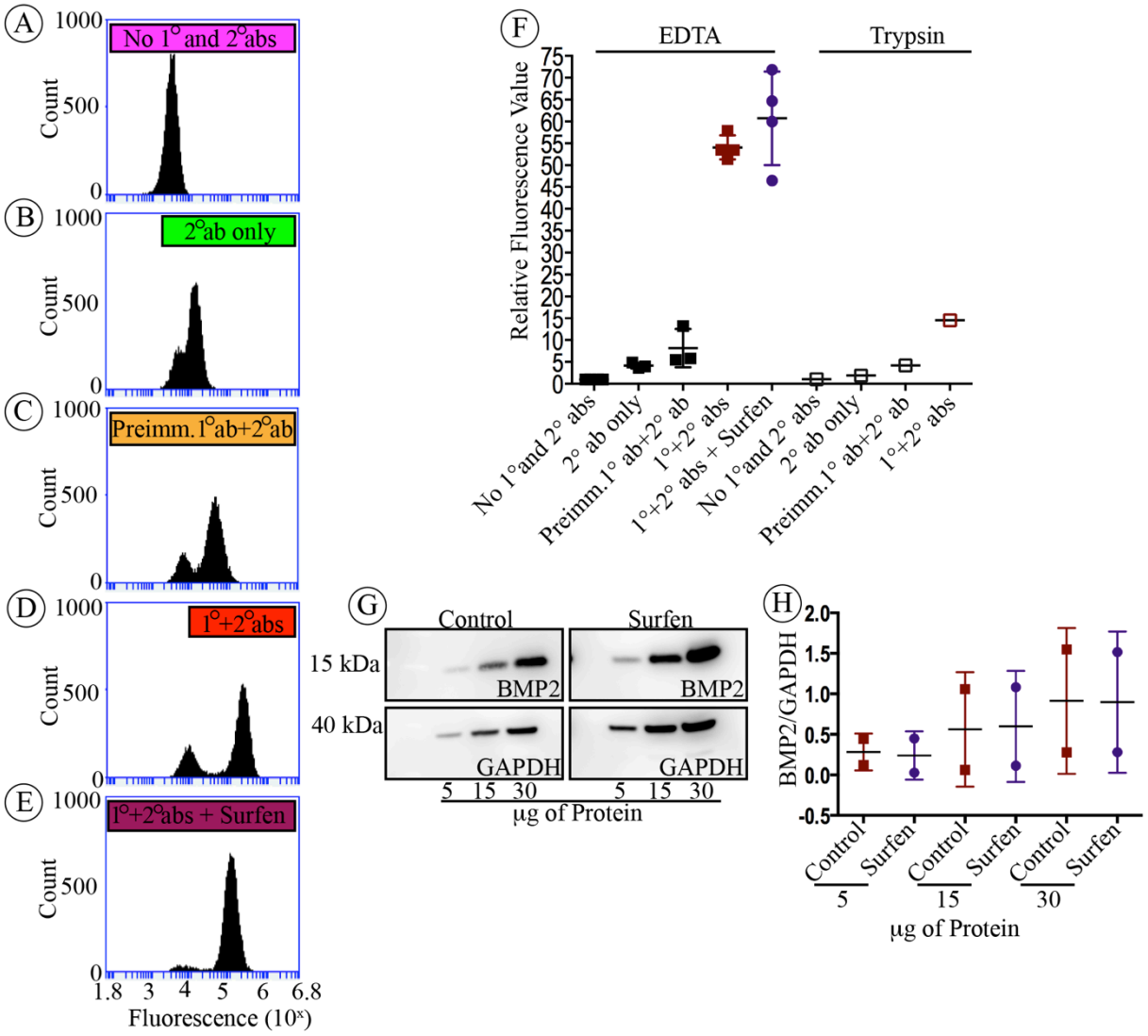
A
No 1° and 2°abs
B
2°ab only
C
Preimm.1°ab+2°ab
D
1°+2°abs
E
1°+2°abs + Surfen
Count
1000
500
0
1.8 3 4 5 6 6.8
Fluorescence (10^x)
F
EDTA
Trypsin
Relative Fluorescence Value
No 1°and 2° abs
2° ab only
Preimm.1° ab+2° ab
1°+2° abs
1°+2° abs + Surfen
G
Control
Surfen
15 kDa
40 kDa
BMP2
GAPDH
5 15 30
µg of Protein
H
BMP2/GAPDH
Control
Surfen
µg of Protein

Figure 3

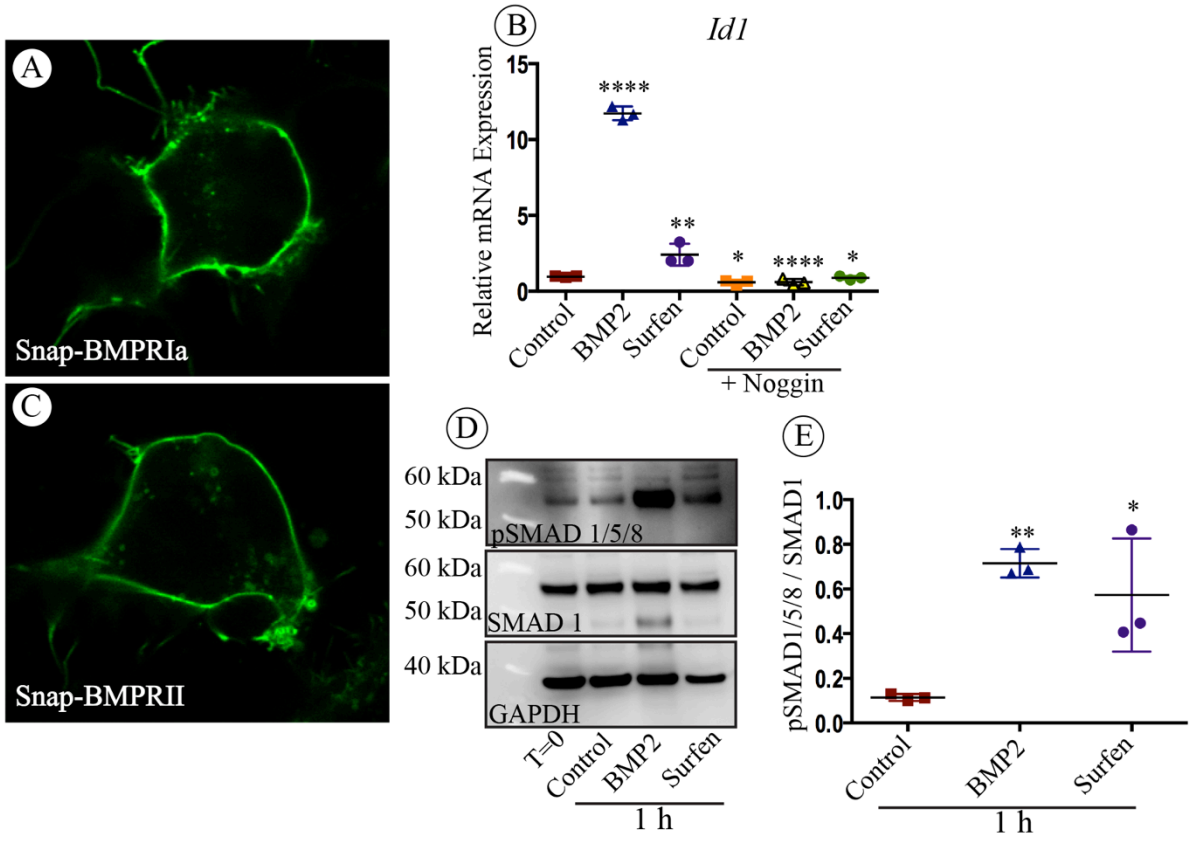

Figure 3

Figure 4

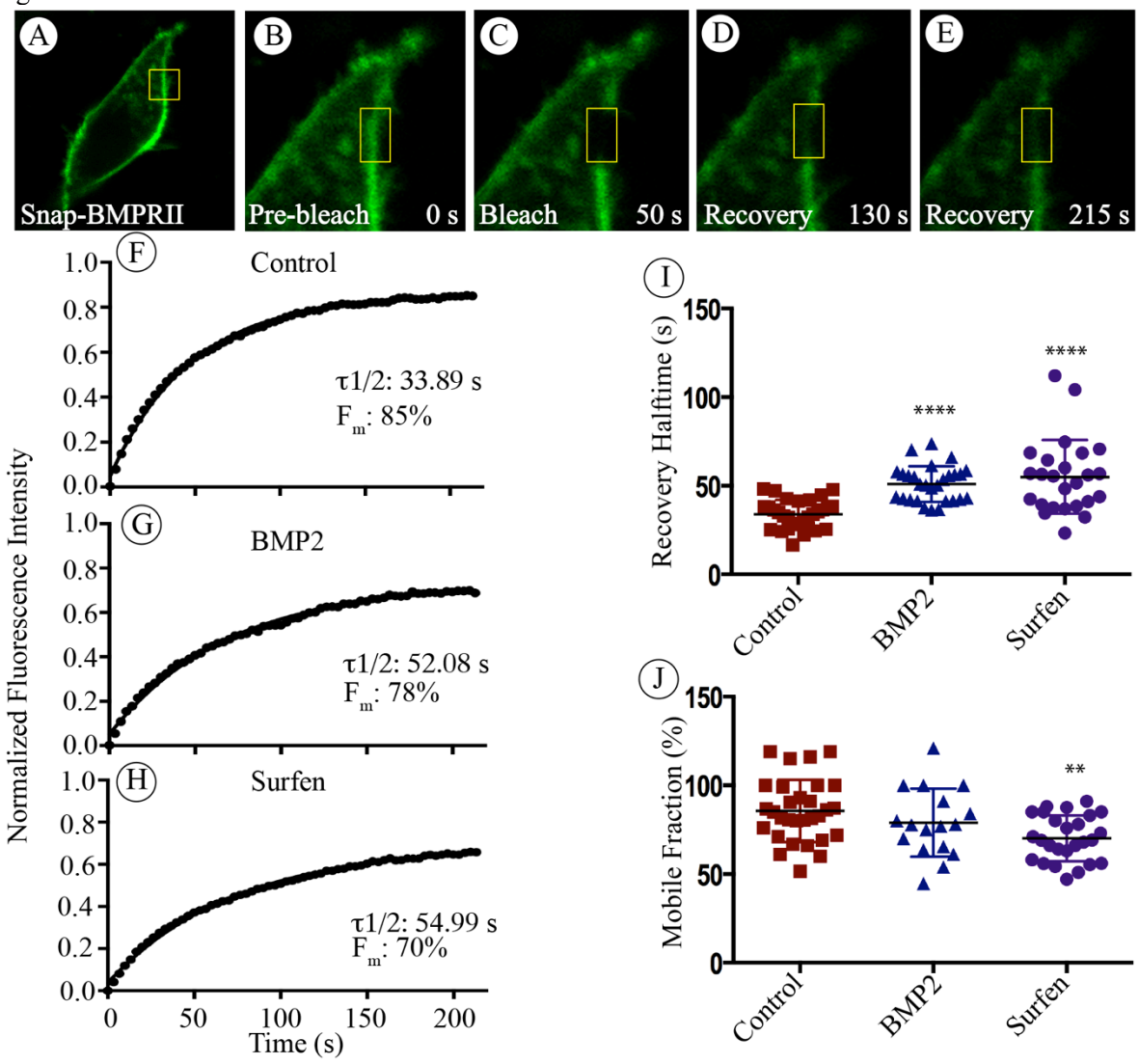
A
Snap-BMPRII
B
Pre-bleach
0 s
C
Bleach
50 s
D
Recovery
130 s
E
Recovery
215 s
F
Control
τ1/2: 33.89 s
F_m: 85%
G
BMP2
τ1/2: 52.08 s
F_m: 78%
H
Surfen
τ1/2: 54.99 s
F_m: 70%
Normalized Fluorescence Intensity
Time (s)
I
Recovery Halftime (s)
****
****
Control
BMP2
Surfen
J
Mobile Fraction (%)
**
Control
BMP2
Surfen

Figure 5

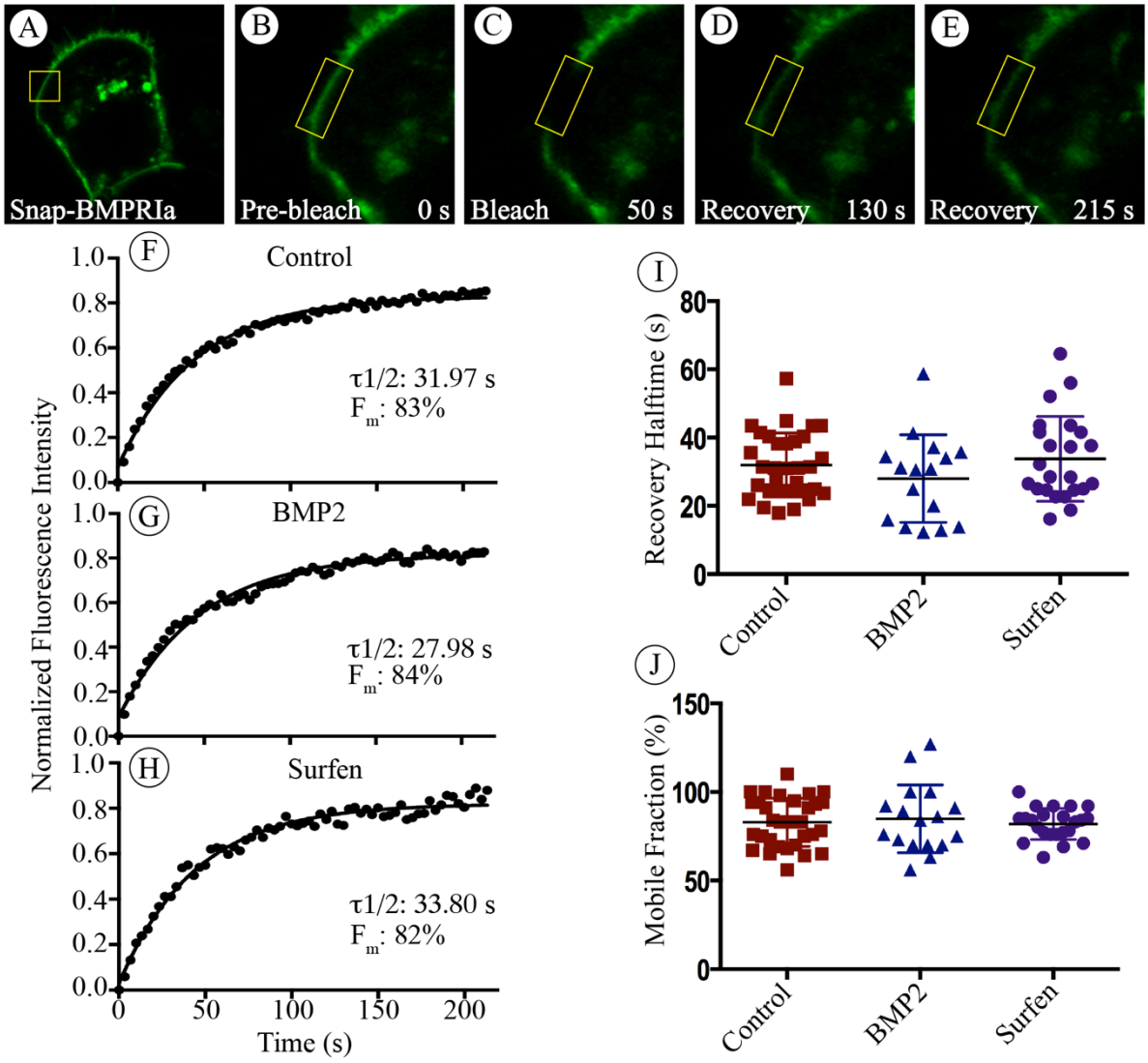
A
B
C
D
E
Snap-BMPRIa
Pre-bleach 0 s
Bleach 50 s
Recovery 130 s
Recovery 215 s
F
Control
τ1/2: 31.97 s
F_m: 83%
G
BMP2
τ1/2: 27.98 s
F_m: 84%
H
Surfen
τ1/2: 33.80 s
F_m: 82%
Normalized Fluorescence Intensity
Time (s)
I
Recovery Halftime (s)
J
Mobile Fraction (%)
Control
BMP2
Surfen

Figure 6

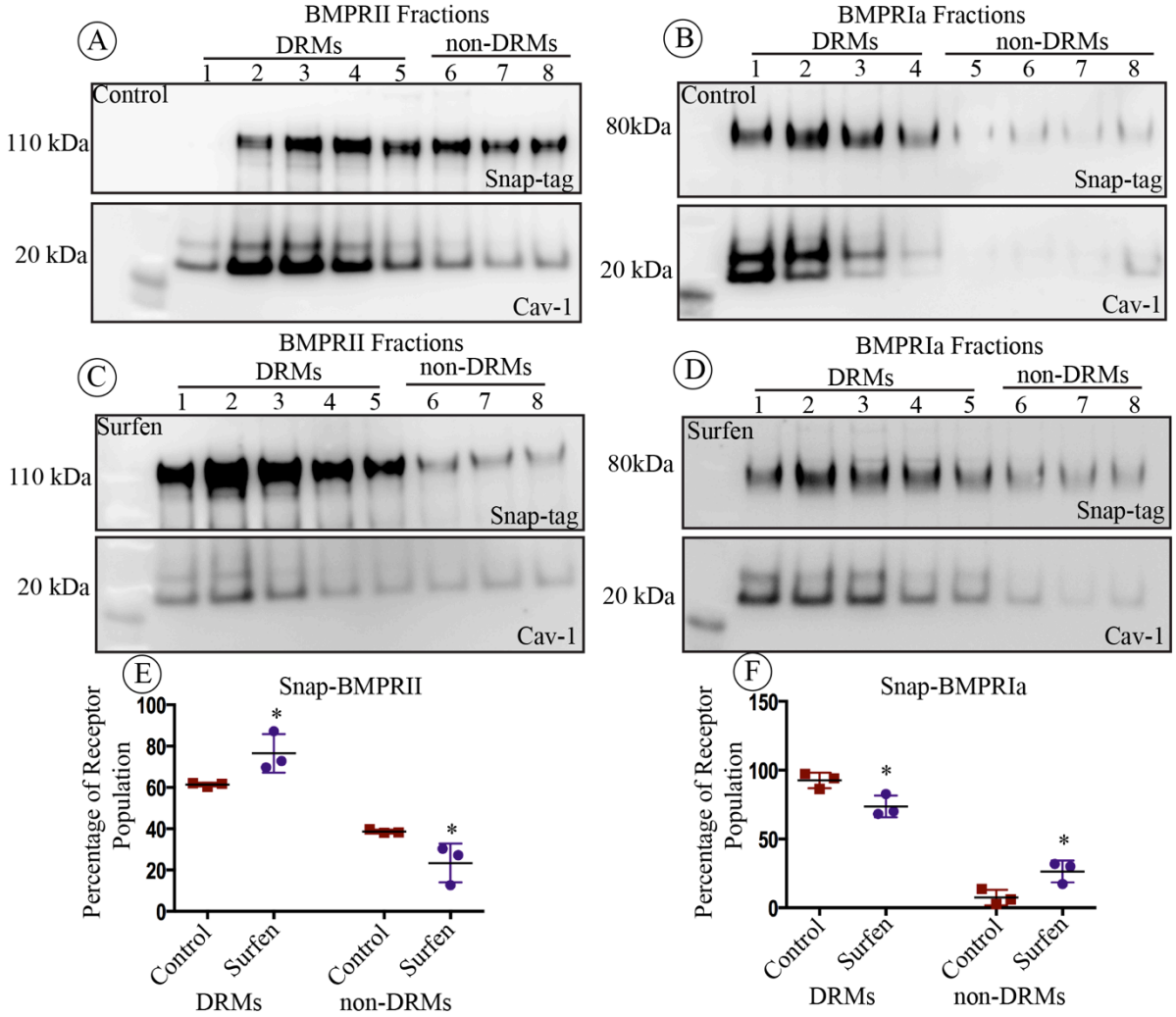
A
BMPRII Fractions
DRMs
non-DRMs
1 2 3 4 5 6 7 8
Control
110 kDa
Snap-tag
20 kDa
Cav-1
B
BMPRIa Fractions
DRMs
non-DRMs
1 2 3 4 5 6 7 8
Control
80kDa
Snap-tag
20 kDa
Cav-1
C
BMPRII Fractions
DRMs
non-DRMs
1 2 3 4 5 6 7 8
Surfen
110 kDa
Snap-tag
20 kDa
Cav-1
D
BMPRIa Fractions
DRMs
non-DRMs
1 2 3 4 5 6 7 8
Surfen
80kDa
Snap-tag
20 kDa
Cav-1
E
Snap-BMPRII
Percentage of Receptor Population
100
80
60
40
20
0
*
*
Control
Surfen
Control
Surfen
DRMs
non-DRMs
F
Snap-BMPRIa
Percentage of Receptor Population
150
100
50
0
*
*
Control
Surfen
Control
Surfen
DRMs
non-DRMs

Figure 7

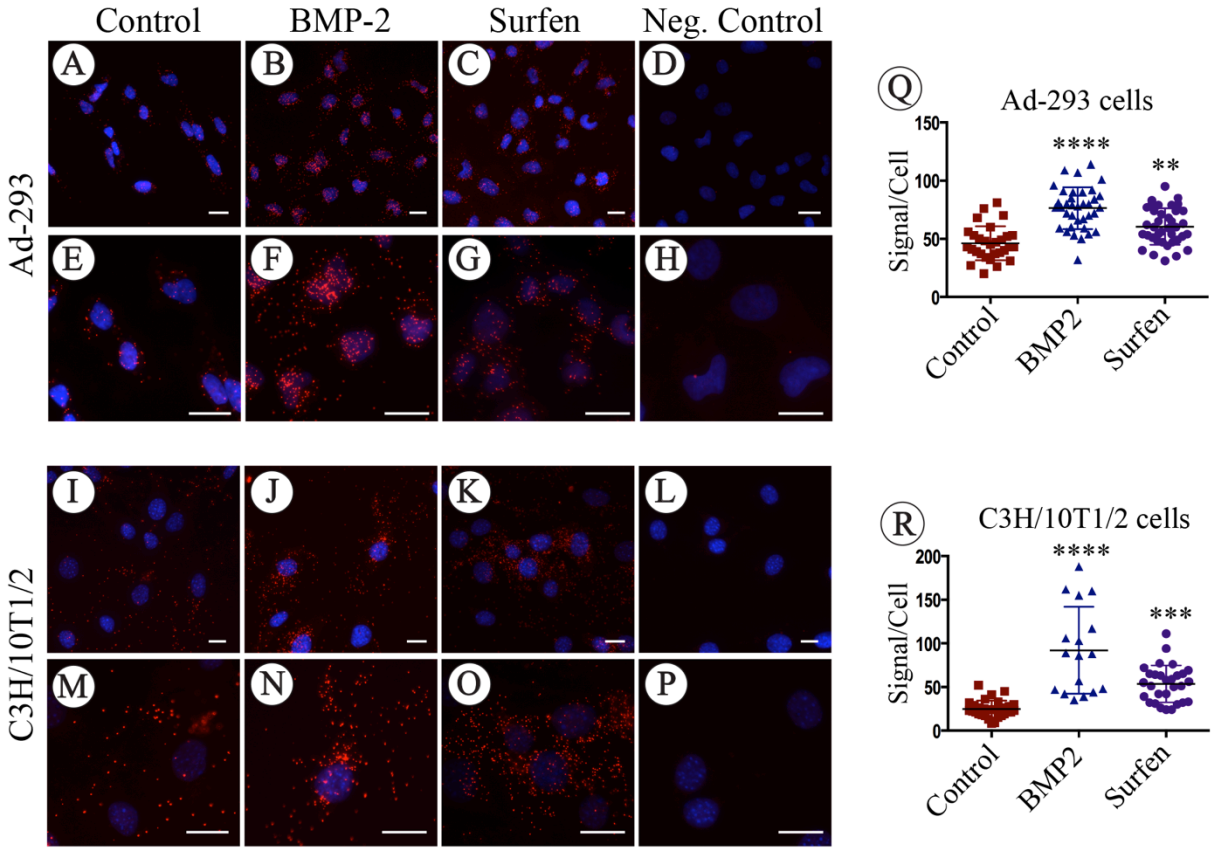
Control
BMP-2
Surfen
Neg. Control
Ad-293
C3H/10T1/2
A
B
C
D
E
F
G
H
I
J
K
L
M
N
O
P
Q
Ad-293 cells
Signal/Cell
150
100
50
0
****
**
Control
BMP2
Surfen
R
C3H/10T1/2 cells
200
150
100
50
0
****
***
Control
BMP2
Surfen

Figure 8

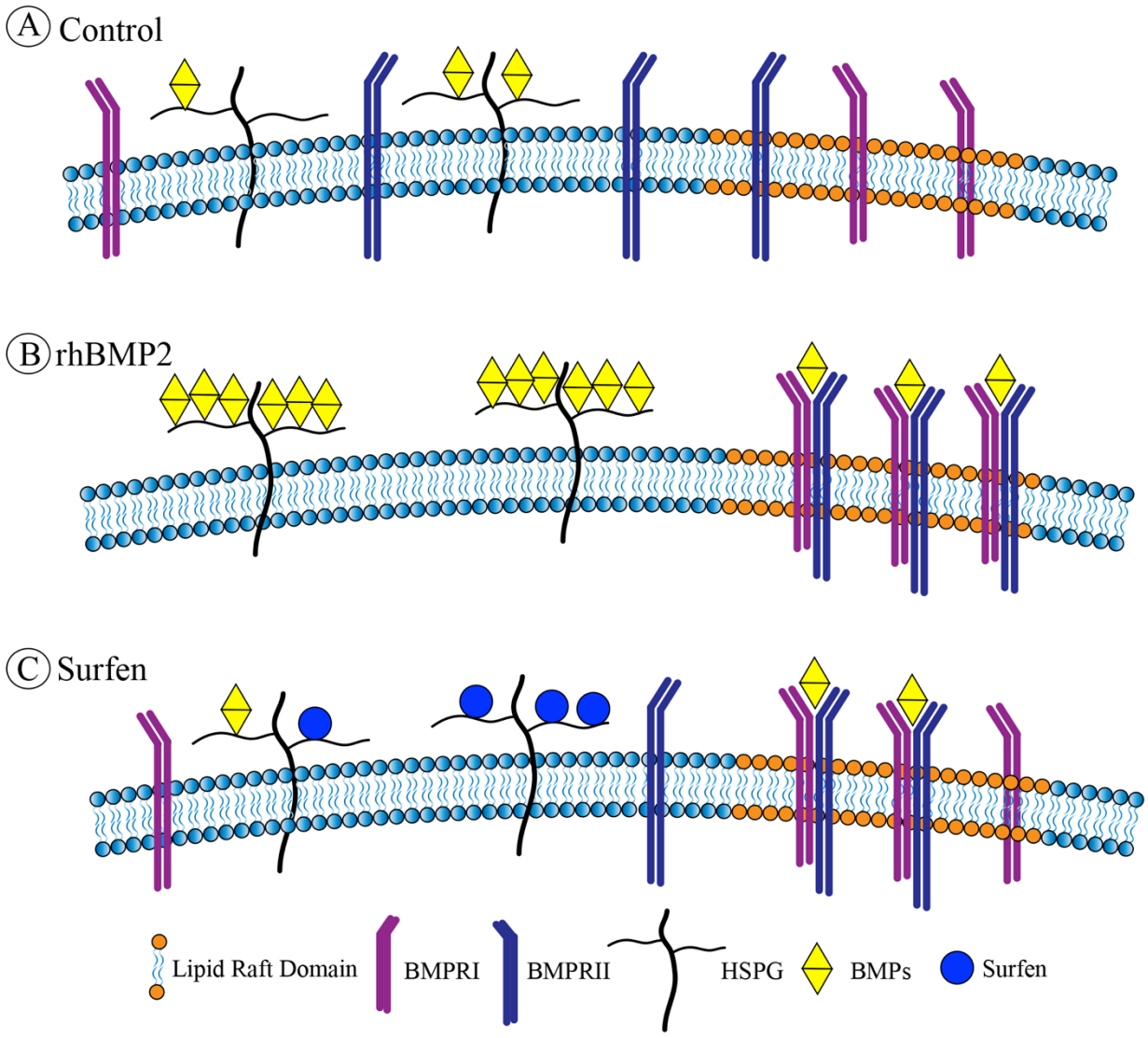
A Control
B rhBMP2
C Surfen
Lipid Raft Domain
BMPRI
BMPRII
HSPG
BMPs
Surfen

Heparan sulfate antagonism alters bone morphogenetic protein signaling and receptor dynamics, suggesting a mechanism in Hereditary Multiple Exostoses

Christina Mundy, Evan Yang, Hajime Takano, Paul C. Billings and Maurizio Pacifici

J. Biol. Chem. published online April 5, 2018
